Project No. 037005

CECILIA

Central and Eastern Europe Climate Change Impact and Vulnerability Assessment

Specific targeted research project

1.1.6.3.I.3.2: Climate change impacts in central-eastern Europe

D4.6
Report and/or peer-reviewed papers documenting the WP4 studies

Due date of deliverable: 31st December 2009
Actual submission date: 30th March 2010

Start date of project: 1st June 2006 Duration: 43 months

Lead contractor for this deliverable: ETH

Project co-funded by the European Commission within the Sixth Framework Programme		
Dissemination Level		
PU	Public	X
PP	Restricted to other programme participants (including the Commission Services)	
RE	Restricted to a group specified by the consortium (including the Commission	
CO	Confidential, only for members of the consortium (including the Commission Services)	

1. Introduction

The purpose of this deliverable is to provide an overview on main results, reports, and publications from CECILIA WP4. In Section 2., we provide an overview of the CECILIA extreme database, which is a main output from the project to which most WP4 participants contributed either through the computation of indices, or the providing of observational and/or modeling data. Furthermore, results and publications from single partners are summarized in Section 3.

2. CECILIA extreme database

A main activity led by ETH Zurich together with DMI and CHMI consisted in the extreme database that was put together in the course of the project as part of deliverables D4.1-D4.4. Based on the list of climate and extreme weather indices that was defined in deliverable D4.1, ETH, DMI and CHMI worked on the implementation of the final list of 154 indices (131 main indices with 23 variants for some indices, see Tables 2.1 and 2.2) in three software tools (R, Matlab, and ProClimDB, respectively). These tools were used by the WP4 partners to compute the indices from the climate model outputs (PRUDENCE, ENSEMBLES, CECILIA simulations) and from the observational data sets (ECA&D, local observations from the WP4 partners, see Fig. 2.1). Moreover, significant effort was invested in order to make the calculation of the indices in the three software tools compatible, and to ensure the consistent computation of the indices from the various data sources. The database is stored at DMI at the following location: http://cecilia.dmi.dk/. It will be made publicly available after the publication of the CECILIA special issue. An article will document the list of considered indices and provide first analyses of the computed data (Seneviratne et al. 2010, in preparation for CECILIA special issue).

The CECILIA extreme database constitutes a major achievement of the WP4 activities. Indeed, it was possible to include a very large number of indices within the database, which comprehensively capture statistical characteristics of temperature and precipitation data in Central and Eastern Europe. The computation of indices was applied to a large number of meteorological stations from the individual partners, for which no raw data could be previously shared. This is illustrated in Fig. 2.1, which displays the density of station data considered within the CECILIA extreme database compared to the density of stations for which raw temperature and precipitation data is available from the ECA&D project.

As an example of some of the analyses that will be provided in the CECILIA special issue, Figs. 2.2 and 2.3 display the comparison of temperature indices from the database for modeling and observational data (see also D4.4 for more details).

Beside the overview publication prepared for the special issue several other publications will result from the analysis of this database (e.g. Hirschi et al. 2010, in prep, see Section 3.1, and Christensen et al. 2010, in prep, see Section 3.2).

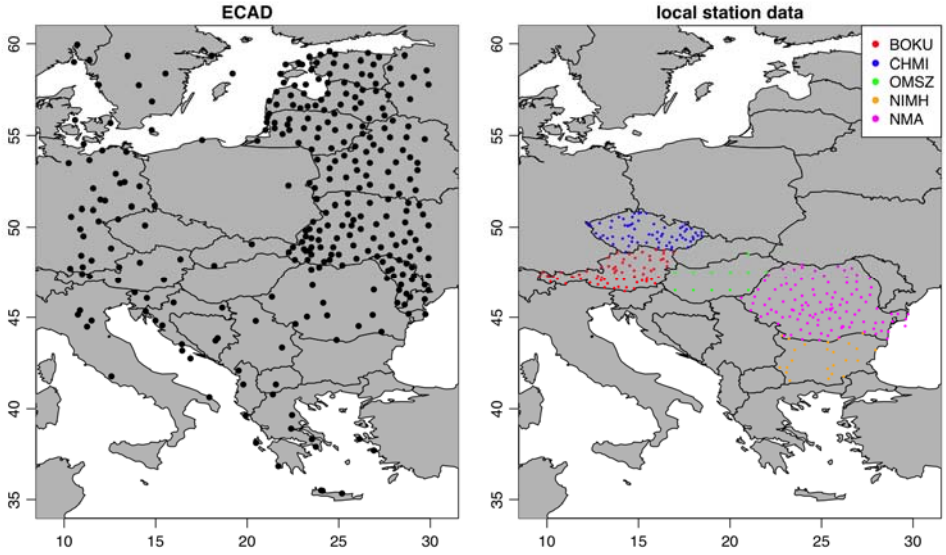

Figure 2.1: *Ground observations considered in the CECILIA extreme database: (left) ECA&D data base; (right) stations from local partners (for Hungary, the data is available on a grid).*

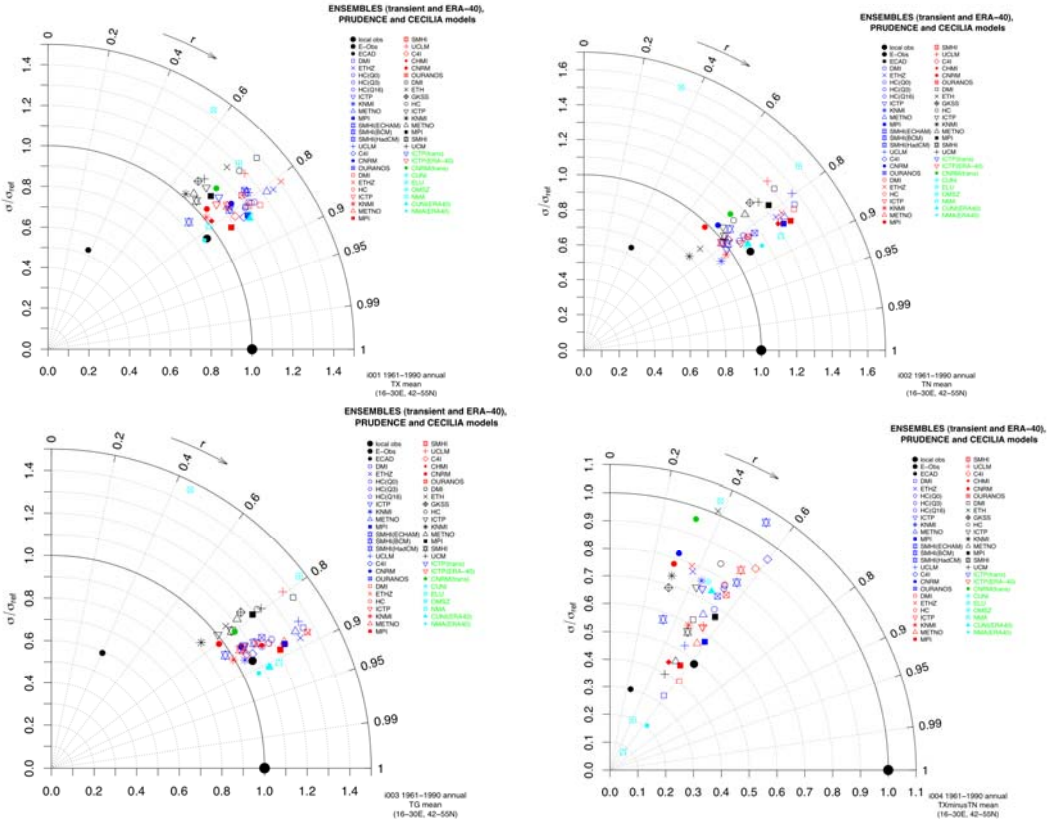

Figure 2.2. *Taylor plots including the ENSEMBLES transient (blue symbols) and ERA-40 (red symbols) simulations, the PRUDENCE RCMs (black symbols), as well as the CECILIA driving and high-resolution runs (green model acronyms, cyan symbols for the high-resolution runs) compared against the local observations. For comparison, also the ECA&D and the E-Obs observations are included (also relative to the local observations). The CECILIA driving runs from ICTP coincide with the respective ENSEMBLES runs and consequently share the same symbols and colors. (Top left) maximum temperature, (top right) minimum temperature, (bottom left) mean temperature, (bottom right) daily temperature range. Displayed are annual values for the period 1961–1990 and for the East European domain (16°E–30°E, 44°N–55°N).* σ *denotes the spatial standard deviations (normalized by the standard deviation of the observations) and r the correlation coefficients.*

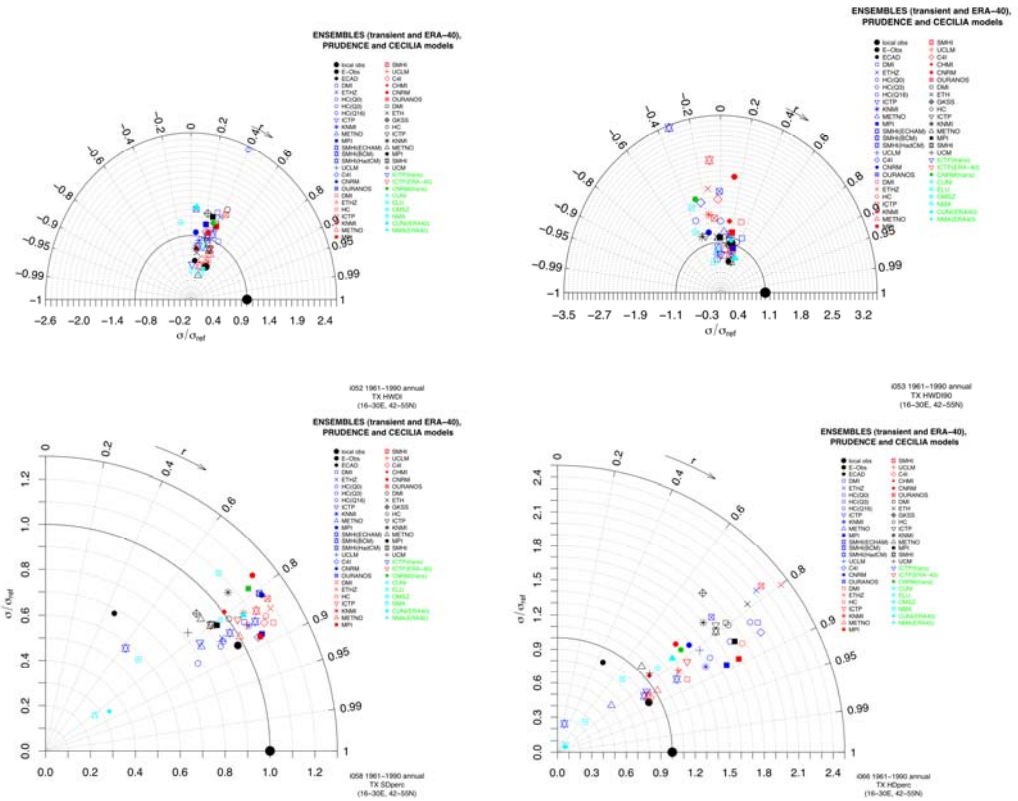

Figure 2.3. *As Figure 2.2, but for two different heat wave indices, i.e., (top left) mean heat wave occurrence and (top right) 90th percentile-based maximum heat wave duration, as well as for (bottom left) percentage of summer days and (bottom right) percentage of hot days.*

Table 2.1: *List of CECILIA WP4 temperature indices*[1]

Temperature indices computed over all time frames							
	Index	**A**	**B**	**C**	**D**	**E**	**Definition**
1	**Mean Tmax**	**X**				**x**	**daily max T° averaged over time frame**
2	**Mean Tmin**	**X**				**x**	**daily min T° averaged over time frame**
3	**Mean Tmean**	**X**				**x**	**daily mean T° averaged over time frame**
4	**Mean DTR**	**X**			**(x)**	**x**	**daily values of (Tmax-Tmin) averaged over time frame**
5	10th percentile DTR	X					10th %ile of daily values of (Tmax-Tmin) within given time frame
6	90th percentile DTR	X					90th %ile of daily values of (Tmax-Tmin) within given time frame
7	Tmax 1st percentile						1st %ile of daily values of Tmax within given time frame
8	Tmax 5th percentile						5th %ile of daily values of Tmax within given time frame
9	Tmax 10th percentile	X					10th %ile of daily values of Tmax within given time frame
10	Tmax 20th percentile						20th %ile of daily values of Tmax within given time frame
11	Tmax 30th percentile						30th %ile of daily values of Tmax within given time frame
12	Tmax 40th percentile						40th %ile of daily values of Tmax within given time frame
13	Tmax 50th percentile						50th %ile of daily values of Tmax within given time frame
14	Tmax 60th percentile						60th %ile of daily values of Tmax within given time frame
15	Tmax 70th percentile						70th %ile of daily values of Tmax within given time frame
16	Tmax 80th percentile						80th %ile of daily values of Tmax within given time frame
17	Tmax 90th percentile	X	X				90th %ile of daily values of Tmax within given time frame
18	Tmax 95th percentile						95th %ile of daily values of Tmax within given time frame
19	Tmax 99th percentile						99th %ile of daily values of Tmax within given time frame
20	Tmean 1st percentile						1st %ile of daily values of Tmean within given time frame
21	Tmean 5th percentile						5th %ile of daily values of Tmean within given time frame
22	Tmean 10th percentile						10th %ile of daily values of Tmean within given time frame
23	Tmean 20th percentile						20th %ile of daily values of Tmean within given time frame
24	Tmean 30th percentile						30th %ile of daily values of Tmean within given time frame

25	Tmean 40th percentile						40th %ile of daily values of Tmean within given time frame
26	Tmean 50th percentile						50th %ile of daily values of Tmean within given time frame
27	Tmean 60th percentile						60th %ile of daily values of Tmean within given time frame
28	Tmean 70th percentile						70th %ile of daily values of Tmean within given time frame
29	Tmean 80th percentile						80th %ile of daily values of Tmean within given time frame
30	Tmean 90th percentile						90th %ile of daily values of Tmean within given time frame
31	Tmean 95th percentile						95th %ile of daily values of Tmean within given time frame
32	Tmean 99th percentile						99th %ile of daily values of Tmean within given time frame
33	Tmin 1st percentile						1st %ile of daily values of Tmin within given time frame
34	Tmin 5th percentile						5th %ile of daily values of Tmin within given time frame
35	Tmin 10th percentile	X	X				10th %ile of daily values of Tmin within given time frame
36	Tmin 20th percentile						20th %ile of daily values of Tmin within given time frame
37	Tmin 30th percentile						30th %ile of daily values of Tmin within given time frame
38	Tmin 40th percentile						40th %ile of daily values of Tmin within given time frame
39	Tmin 50th percentile						50th %ile of daily values of Tmin within given time frame
40	Tmin 60th percentile						60th %ile of daily values of Tmin within given time frame
41	Tmin 70th percentile						70th %ile of daily values of Tmin within given time frame
42	Tmin 80th percentile						80th %ile of daily values of Tmin within given time frame
43	Tmin 90th percentile	X					90th %ile of daily values of Tmin within given time frame
44	Tmin 95th percentile						95th %ile of daily values of Tmin within given time frame
45	Tmin 99th percentile						99th %ile of daily values of Tmin within given time frame
46	**Percentage of frost days**	**(x)**	**(x)**	**(x)**	**(x)**	**(x)**	**%age of days within time frame with Tmin < 0C (ECA&D Number of frost days)**
46a	**Days with freezing-point passage**						**%age of days within time frame with Tmin<0C and Tmax>0C**
47	**Percentage of days without defrost (ice days)**	**(x)**			**(x)**	**(x)**	**%age of days within time frame with Tmax < 0C (ECA&D: Number of ice days)**
48	***Consecutive frost days***					***x***	***Max. nb of consecutive frost days with Tmin < 0C. Lengths limited to the relevant time frame***
48f	***Consecutive frost days***					***x***	***Max. nb of consecutive frost days with Tmin < 0C. Full lengths considered***
49	***Growing degree days (def1)***	***X***				***x***	***Sum of (Tmean-4C) for all days with Tmean>4C within time frame (ECA definition)***
50	*Growing degree days (def2)*						*Sum of (((Tmax+Tmin)/2)-10C) for all days with Tmax≥10C within time frame using the following rules: if Tmin<10C, then use 10C for Tmin; if Tmax>30C then use 30C for Tmax*
51	***Extreme temperature range within time frame***	***(x)***		***(x)***		***(x)***	***Range between max. Tmax and min. Tmin within time frame (for annual time frame equivalent to intra-annual extreme temperature range)***
52	**Mean heat wave occurrence**	**X**		**x**		**x**	**Let Tx_{ij} be the daily maximum temperature at day *i* of period *j* and let Tx_{inorm} be the calendar day mean calculated for a 5 day window centred on each calendar day during a specified period. Then counted is the percentage of days per period where, in intervals of at least 6 consecutive days: $Tx_{ij} > Tx_{inorm} + 5$ (adapted from STARDEX definition). Lengths limited to the relevant time frame (spells considered need to have a minimum of 6 days within the given time frame).**
52f	**Mean heat wave occurrence (full spell lengths)**	**X**		**x**		**x**	**Let Tx_{ij} be the daily maximum temperature at day *i* of period *j* and let Tx_{inorm} be the calendar day mean calculated for a 5 day window centred on each calendar day during a specified period. Then counted is the percentage of days per period where, in intervals of at least 6 consecutive days: $Tx_{ij} > Tx_{inorm} + 5$ (adapted from STARDEX definition). Full lengths considered (spells considered may be only partially within time frame; but only days within period are summed)**
52a	**Mean heat wave length**						**Day-weighted average of spell lengths of at least 6 days as defined in 52. Lengths limited to the relevant time frame .**
52af	**Mean heat wave length (full spell lengths)**						**Day-weighted average of spells of at least 6 days as defined in 52. Full lengths considered.**

53	**90th percentile-based maximum heat wave duration**	**X**	**X**				**Let Tx_{ij} be the daily maximum temperature at day *i* of period *j* and let $Txq90_{inorm}$ be the calendar day 90th percentile calculated for a 5 day window centred on each calendar day during a specified period. Then counted is the maximum number of consecutive days per period where: $T_{ij} > Txq90_{inorm}$ (adapted from STARDEX definition). Lengths limited to the relevant time frame .**
53f	**90th percentile-based maximum heat wave duration (full spell lengths)**	**X**	**x**				**Let Tx_{ij} be the daily maximum temperature at day *i* of period *j* and let $Txq90_{inorm}$ be the calendar day 90th percentile calculated for a 5 day window centred on each calendar day during a specified period. Then counted is the maximum number of consecutive days per period where: $T_{ij} > Txq90_{inorm}$ (adapted from STARDEX definition). Full length considered.**
53a	**90th percentile-based mean heat wave length**						**Day-weighted average of spells lengths of at least 2 days as defined in 53. Lengths limited to the relevant time frame .**
53af	**90th percentile-based mean heat wave length (full spell lengths)**						**Day-weighted average of spells of at least 2 days as defined in 53. Full lengths considered.**
54	***Heating degree days***					***x***	***Sum of 17C-Tmean for days with Tmean<17C***
55	**Mean cold wave occurrence**	**X**				**x**	**Let Tn_{ij} be the daily minimum temperature at day *i* of period *j* and let Tn_{inorm} be the calendar day mean calculated for a 5 day window centred on each calendar day during a specified period. Then counted is the percentage of days per period where, in intervals of at least 6 consecutive days: $Tn_{ij} < Tn_{inorm} - 5$ (adapted from STARDEX definition). Lengths limited to the relevant time frame .**
55f	**Mean cold wave occurrence (full spell lengths)**	**X**				**x**	**Let Tn_{ij} be the daily minimum temperature at day *i* of period *j* and let Tn_{inorm} be the calendar day mean calculated for a 5 day window centred on each calendar day during a specified period. Then counted is the percentage of days per period where, in intervals of at least 6 consecutive days: $Tn_{ij} < Tn_{inorm} - 5$ (adapted from STARDEX definition). Full length considered**
55a	**Mean cold wave length**						**Day-weighted average of spells of at least 2 days as defined in 55. Lengths limited to the relevant time frame .**
55af	**Mean cold wave length (full spell lengths)**						**Day-weighted average of spells of at least 2 days as defined in 55. Full lengths considered.**
56	**10th percentile-based maximum cold wave duration**	**X**					**Let Tn_{ij} be the daily minimum temperature at day *i* of period *j* and let $Tnq10_{inorm}$ be the calendar day 10th percentile calculated for a 5 day window centred on each calendar day during a specified period. Then counted is the maximum number of consecutive days per period where: $Tn_{ij} < Tnq10_{inorm}$ (adapted from STARDEX def.). Lengths limited to the relevant time frame .**
56f	**10th percentile-based maximum cold wave duration (full spell lengths)**	**X**					**Let Tn_{ij} be the daily minimum temperature at day *i* of period *j* and let $Tnq10_{inorm}$ be the calendar day 10th percentile calculated for a 5 day window centred on each calendar day during a specified period. Then counted is the maximum number of consecutive days per period where: $Tn_{ij} < Tnq10_{inorm}$ (adapted from STARDEX def.). Full length considered**
56a	**10th percentile-based cold wave length**						**Day-weighted average of spells of at least 2 days as defined in 56. Lengths limited to the relevant time frame.**
56af	**10th percentile-based mean cold wave length (full spell lengths)**						**Day-weighted average of spells of at least 2 days as defined in 56. Full lengths considered.**
57	Frost season length	(x)					Mean duration within time frame of time spans of minimum 5 consecutive days where Tmin<0 (adapted from STARDEX definition). Day-weighted. Length limited to the relevant time frame .
57f	Frost season length (full spell lengths)	(x)					Mean duration within time frame of time spans of minimum 5 consecutive days where Tmin<0 (adapted from STARDEX definition). Day-weighted. Full length of spell considered.

58	**Percentage of "summer days"**				**(x)**	**(x)**	**%age of days where Tmax ≥ 25C**
59	**Percentage of "tropical nights"**				**(x)**	**(x)**	**%age of days where Tmin ≥ 20C**
60	**Percentage of days with Tmax < 10th percentile**	**X**		**x**	**x**	**x**	**%age of days with Tmax < 10th percentile, where 10th percentile is taken from all values for 5-day window around calendar day within base period (ECA&D def.)**
61	**Percentage of days with Tmax > 90th percentile**	**X**		**x**	**x**	**x**	**%age of days with Tmax > 90th percentile, where 90th percentile is taken from all values for 5-day window around calendar day within base period (ECA&D def.)**
62	**Percentage of days with Tmean < 10th percentile**					**x**	**%age of days with Tmean < 10th percentile, where 10th percentile is taken from all values for 5-day window around calendar day within base period (ECA&D def)**
63	**Percentage of days with Tmean > 90th percentile**					**x**	**%age of days with Tmean > 90th percentile, where 90th percentile is taken from all values for 5-day window around calendar day within base period (ECA&D def.)**
64	**Percentage of days with Tmin < 10th percentile**	**X**		**x**	**x**	**x**	**%age of days with Tmin < 10th percentile, where 10th percentile is taken from all values for 5-day window around calendar day within base period (ECA&D def.)**
65	**Percentage of days with Tmin > 90th percentile**	**X**		**x**	**x**	**x**	**%age of days with Tmin > 90th percentile, where 90th percentile is taken from all values for 5-day window around calendar day within base period (ECA&D def.)**
66	**Percentage of hot days**						**%age of days with Tmax ≥ 30C (adapted from ELU definition)**
67	Percentage of extremely hot days						%age of days with Tmax ≥ 35C (adapted from ELU definition)
68	Percentage of severe cold days						%age of days with Tmin < -10C (adapted from ELU definition)
69	Interannual variability of Tmean						Standard deviation of mean yearly values of Tmean averaged over given time frame (e.g. month)
70	Interannual variability of Tmax						Standard deviation of mean yearly values of Tmax averaged over given time frame (e.g. month)
71	Interannual variability of Tmin						Standard deviation of mean yearly values of Tmin averaged over given time frame (e.g. month)
72	Intra-annual variability of Tmean						Mean over whole time period (e.g. 10-yr period) of yearly standard deviation of Tmean within given time frame
73	Intra-annual variability of Tmax						Mean over whole time period (e.g. 10-yr period) of yearly standard deviation of Tmean within given time frame
74	Intra-annual variability of Tmin						Mean over whole time period (e.g. 10-yr period) of yearly standard deviation of Tmean within given time frame
Temperature indices computed only over annual time frames							
	Index	**A**	**B**	**C**	**D**	**E**	**Definition**
75	***Growing season length***	***X***		***x***	***x***	***x***	***Annual count between first span of at least 6 days with daily mean temperature Tmean>5C (counting starts on the first day of this span) and first span after July 1st of 6 days with Tmean<5C (counting stops on the last day before this span) (RClimDex definition).***

[1]Comments on Table 2.1:

- "time frame" refers to annual, seasonal, and monthly time frames
- **The indices denoted in bold face are provided as yearly output ("core indices")**
- Indices in standard font: this index is computed from the total number of available days over all years (i.e. for a monthly time frame and a 10-year time period, from 300 values)
- *Indices in italic: this index is computed separately for each year and averaged over all years (i.e. for a monthly time frame and a 10-year time period, mean of 10 values, each one of which is computed from 30 values)*
- Indices in gray: indices with special definition

Table 2.2: *List of CECILIA WP4 precipitation indices*[2]

Precipitation indices computed over all time frames							
	Index	**A**	**B**	**C**	**D**	**E**	**Definition**
76	**Mean climatological precipitation**	**X**				**x**	**Mean precipitation (including both wet and dry days)**
77	**Mean wet-day precip.**	**X**	**x**	**x**	**x**	**x**	**Mean wet-day precipitation (equivalent to "simple daily intensity")**
78	**Percentage of wet days**					**x**	**Nb wet days/ total nb of days [%]**
79	10th %ile wet-day						10th %ile of wet-day amounts [mm/d]

	amounts						
80	20th %ile wet-day amounts	X					20th %ile of wet-day amounts [mm/d]
81	30th %ile wet-day amounts						30th %ile of wet-day amounts [mm/d]
82	40th %ile wet-day amounts	X					40th %ile of wet-day amounts [mm/d]
83	50th %ile wet-day amounts	X					50th %ile of wet-day amounts [mm/d]
84	60th %ile wet-day amounts	X					60th %ile of wet-day amounts [mm/d]
85	70th %ile wet-day amounts						70th %ile of wet-day amounts [mm/d]
86	80th %ile wet-day amounts	X					80th %ile of wet-day amounts [mm/d]
87	90th %ile wet-day amounts	X	x				90th %ile of wet-day amounts [mm/d]
88	95th %ile wet-day amounts	X					95th %ile of wet-day amounts [mm/d]
89	99th %ile wet-day amounts						99th %ile of wet-day amounts [mm/d]
90	*Fraction of total precip. above annual 10th %ile*						*Fraction of total precipitation above annual 10th percentile (sum and percentile based on wet-day amounts)*
91	*Fraction of total precip. above annual 20th %ile*	*X*					*Fraction of total precipitation above annual 20th percentile (sum and percentile based on wet-day amounts)*
92	*Fraction of total precip. above annual 30th %ile*						*Fraction of total precipitation above annual 30th percentile (sum and percentile based on wet-day amounts)*
93	*Fraction of total precip. above annual 40th %ile*	*X*					*Fraction of total precipitation above annual 40th percentile (sum and percentile based on wet-day amounts)*
94	*Fraction of total precip. above annual 50th %ile*	*X*					*Fraction of total precipitation above annual 50th percentile (sum and percentile based on wet-day amounts)*
95	*Fraction of total precip. above annual 60th %ile*	*X*					*Fraction of total precipitation above annual 60th percentile (sum and percentile based on wet-day amounts)*
96	*Fraction of total precip. above annual 70th %ile*						*Fraction of total precipitation above annual 70th percentile (sum and percentile based on wet-day amounts)*
97	*Fraction of total precip. above annual 80th %ile*	*X*					*Fraction of total precipitation above annual 80th percentile (sum and percentile based on wet-day amounts)*
98	***Fraction of total precip. above annual 90th %ile***	***X***					***Fraction of total precipitation above annual 90th percentile (sum and percentile based on wet-day amounts)***
99	***Fraction of total precip. above annual 95th %ile***	***X***					***Fraction of total precipitation above annual 95th percentile (sum and percentile based on wet-day amounts)***
100	***Fraction of total precip. above annual 99th %ile***						***Fraction of total precipitation above annual 99th percentile (sum and percentile based on wet-day amounts)***
101	**Percentage of wet days above 10 mm/d**	**(x)**		**(x)**	**(x)**	**(x)**	**%age of wet days above 10 mm/d (ECA&D: number of days)**
102	**Percentage of wet days above 20 mm/d**				**(x)**	**(x)**	**%age of wet days above 20 mm/d (ECA&D: number of days)**
103	***Max. nb of consecutive dry days***	***X***	***x***	***x***	***x***	***x***	***Max. nb of consecutive dry days. Length limited to relevant time frame.***
103f	***Max. nb of consecutive dry days (full spell lengths)***	***X***	***x***	***x***	***x***	***x***	***Max. nb of consecutive dry days. Full length considered.***
104	***Max. nb of consecutive wet days***	***X***			***x***	***x***	***Max. nb of consecutive wet days. Length limited to relevant time frame .***
104f	***Max. nb of consecutive wet days (full spell lengths)***	***X***			***x***	***x***	***Max. nb of consecutive wet days. Full length considered.***
105	Mean wet-day persistence	X					Total number of consecutive (at least 2) wet days/Total number of wet days (STARDEX definition)
106	Mean dry-day persistence	X					Total number of consecutive (at least 2) dry days/Total number of dry days
107	**Mean wet spell**	**x**					**Mean wet spell length (days) Length limited to**

	length (days)						**relevant time frame . Day-weighted**
107f	**Mean wet spell length (days) Full spell lengths**	**X**					**Mean wet spell length (days). Full length considered. Day-weighted**
108	Median wet spell length (days)	X					Median wet spell length (days) Length limited to relevant time frame .
108f	Median wet spell length (days) Full spell lengths	X					Median wet spell length (days). Full length considered.
109	Standard deviation of wet spell length (days)	X					Standard deviation of wet spell length (days) Length limited to relevant time frame . Day-weighted.
109f	Standard deviation of wet spell length (days) Full spell lengths	X					Standard deviation of wet spell length (days) Full length considered. Day-weighted.
110	**Mean dry spell length (days)**	**X**					**Mean dry spell length (days) Length limited to relevant time frame . Day-weighted.**
110f	**Mean dry spell length (days) Full spell lengths**	**X**					**Mean dry spell length (days). Full length considered. Day-weighted.**
111	Median dry spell length (days)	X					Median dry spell length (days) Length limited to relevant time frame .
111f	Median dry spell length (days) Full spell lengths	X					Median dry spell length (days). Full length considered.
112	Standard deviation of dry spell length (days)	X					Standard deviation of dry spell length (days) Length limited to relevant time frame . Day-weighted.
112f	Standard deviation of dry spell length (days) Full spell lengths	X					Standard deviation of dry spell length (days). Full length considered.
113	***Greatest 1-day total rainfall***					***x***	***Greatest 1-day total rainfall (ECA&D: max. daily precipitation)***
114	*Greatest 3-day total rainfall*	*X*					*Greatest 3-day total rainfall*
115	***Greatest 5-day total rainfall***	***X***	***x***	***x***		***x***	***Greatest 5-day total rainfall***
116	*Greatest 10-day total rainfall*	*X*					*Greatest 10-day total rainfall*
117	%age of rainfall from events > base-period 90th %ile	X	x				Percentage of rainfall from events > base-period 90th percentile (for given time frame) (based on wet-day amounts)
118	%age of rainfall from events > base-period 95th %ile			(x)	(x)		Percentage of rainfall from events > base-period 95th percentile (for given time frame) (based on wet-day amounts)
119	%age of rainfall from events > base-period 99th %ile						Percentage of rainfall from events > base-period 99th percentile (for given time frame) (based on wet-day amounts)
120	Percentage of wet days > base-period 75th %ile					x	(Nb of wet days > base-period 75th percentile)/Nb of wet days [%] (percentile for given time frame, based on wet-day amounts)
121	**Percentage of wet days > base-period 90th %ile**	**(x)**	**(x)**				**(Nb of wet days > base-period 90th percentile)/Nb of wet days [%] (percentile for given time frame, based on wet-day amounts)**
122	**Percentage of wet days > base-period 95th %ile**					**x**	**(Nb of wet days > base-period 95th percentile)/Nb of wet days [%] (percentile for given time frame, based on wet-day amounts)**
123	**Percentage of wet days > base-period 99th %ile**					**x**	**(Nb of wet days > base-period 99th percentile)/Nb of wet days [%] (percentile for given time frame, based on wet-day amounts)**
124	Percentage of wet days > 20mm						(Nb of wet days > 20mm)/Nb of wet days [%]
125	Percentage of wet days > 10mm						(Nb of wet days > 10mm)/Nb of wet days [%]
126	Percentage of wet days > 5mm						(Nb of wet days > 5mm)/Nb of wet days [%]
127	Interannual variability of mean precipitation						Standard deviation of mean yearly values of precipitation averaged over given time frame (e.g. month)
128	Interannual variability of wet-day precipitation						Standard deviation of mean yearly values of wet-day precipitation averaged over given time frame (e.g. month)
129	Intra-annual variability of mean precipitation						Mean over whole time period (e.g. 10-yr period) of yearly standard deviation of mean precipitation within given time frame

130	Intra-annual variability of wet-day precipitation						Mean over whole time period (e.g. 10-yr period) of yearly standard deviation of wet-day precipitation within given time frame
131	Correlation of (Tmean, Pmean)						Correlation over whole time period (e.g. 10-yr period) between mean temperature and mean precipitation within given time frame

[2]Comments on Table 2.2:

- "time frame" refers to annual, seasonal, and monthly time frames
- **The indices denoted in bold face are provided as yearly output ("core indices")**
- Indices in standard font: this index is computed from the total number of available days over all years (i.e. for a monthly time frame and a 10-year time period, from 300 values)
- *Indices in italic: this index is computed separately for each year and averaged over all years (i.e. for a monthly time frame and a 10-year time period, mean of 10 values, each one of which is computed from 30 values)*
- Indices in gray: indices with special definition

3. Contributions of individual partners

3.1. ETH Zurich

ETH Zurich led WP4 and was involved in all conducted deliverables.

WP4 Deliverables that were prepared by ETH Zurich in the course of the project include the following:

- D4.1 deliverable: Definition of measures and indices to be validated, and selection of observational data sets to be used for the validation of extremes. A detailed implementation plan concerning the analyses to be performed under D4.2, D4.3, D4.4, and D4.5 was issued. (Contributors: All participants)

- D4.3 deliverable: Analyses of CECILIA driving-model simulations. (Contributors: ETH, DMI; AUTH, IAP, and NMA for investigations of links between large-scale circulation patterns and extreme events)

- D4.6 deliverable: present report

Furthermore, several publications have been prepared at ETH Zurich based on or related to CECILIA research. These are summarized in the following subsections. Note that the overview publication on the CECILIA extreme indices and database led by ETH Zurich (Seneviratne et al. 2010) is described in Section 2.

3.1.1. Impact of soil moisture on extremes and trends in regional climate simulations

In this publication (Jaeger and Seneviratne, 2010, in press), the role of soil moisture for extremes and trends in regional climate simulations was investigated as part of deliverable D4.5. For details, please refer to the report on deliverable D4.5. A main result of this study is the identification of asymmetric effects of soil moisture for temperature extremes. This finding is consistent with more recent analyses based on observational indices from the CECILIA database (Section 3.1.2).

3.1.2. Impact of soil moisture deficit on hot extremes analysed from observations

This subsection summarizes results from an ETH study entitled "Observations reveal soil moisture impact on hot extremes in Southeastern Europe", which is in preparation (Hirschi et al. 2010, in prep).

Using quantile regression (Koenker 2005) and the various observational and modeling data sets from the CECILIA indices database, we investigate the relation of hot temperature extremes (as expressed by the indices i001 - Tmax, i061 - TX90p, and i053 - HWDI90 from the data base) with soil moisture deficit (as expressed by the standardized precipitation index, SPI, McKee et al. 1993) in Central and Eastern Europe.

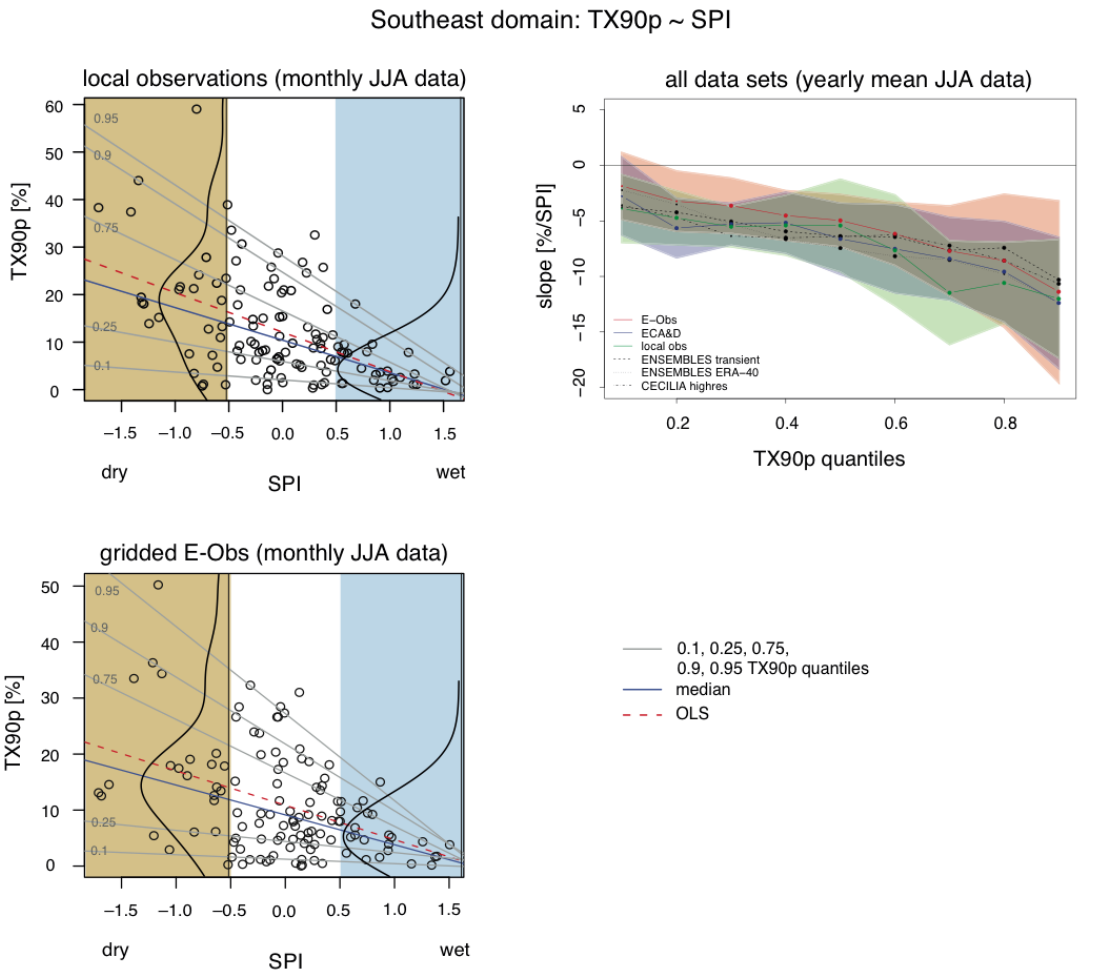

Figure 3.1.1*: (Left panels) Scatter plots of monthly JJA TX90p vs. SPI from the local observations (top) and from the gridded E-Obs (bottom), average values for the Southeast domain and the period 1961-2000. Also shown are estimated PDFs for wet and dry conditions respectively, as well as the regression lines for the ordinary least squares regression (OLS) and for a selection of distinct quantiles (i.e., median, 0.1, 0.25, 0.75, 0.9, 0.95). (Right) Quantile regression slopes of the 0.1-0.9 quantiles of mean yearly JJA TX90p in relation to SPI for the three analysed observational data sets and for the regional climate models. Significant slopes on the 5% significance level (two-tailed test) are denoted with a bold dot. In case of the models, the ensemble median slopes are shown, and dots are displayed as significant when at least 75% of the respective models are significant. Moreover, +/- one standard errors are displayed as shadings for the observational datasets.*

In a Southeast domain (encompassing Bulgaria and Romania) with a soil moisture-limited evapotranspiration regime (Teuling et al., 2009), the analysis reveals that such a relation is in particular present when looking at the upper quantiles of the temperature extreme indices (i.e., the stronger extremes, see Figure 3.1.1, right panel). Such a quantile dependency of the relation is not apparent in the more energy-controlled regime of the Northwest domain (not shown).

These results complement previous modelling studies in the greater European region, showing that the amplification of hot extremes through soil moisture-temperature feedbacks is in particular acting in the transitional zones where soil moisture constrains evapotranspiration variability (Seneviratne et al. 2006; Jaeger and Seneviratne 2010, see also Section 3.1.1).

3.1.3. Other publications

Other WP4-related publications at ETH Zurich include a validation of land-atmosphere coupling characteristics in the COSMO-CLM model with a focus on its implication for the simulation of heat waves (Jaeger et al. 2009), and the investigation of the role of soil moisture memory for the persistence of heat waves (Lorenz et al. 2010, in press).

3.1.4. List of publications in peer-reviewed journals (published, submitted or in preparation)

Hirschi, M., et al., 2010, in prep: Observations reveal soil moisture impact on hot extremes in Southeastern Europe.

Jaeger, E.B., R. Stöckli and S.I. Seneviratne, 2009: Analysis of planetary boundary layer fluxes and land-atmosphere coupling in the Regional Climate Model CLM. J. Geophys. Res. - Atmospheres, 114, D17106.

Jaeger, E.B., and S.I. Seneviratne, 2010: Impact of soil moisture-atmosphere coupling on European climate extremes and trends in a regional climate model. Climate Dynamics, in press.

Lorenz, R., E.B. Jaeger, and S.I. Seneviratne, 2010: Persistence of heat waves and its link to soil moisture memory. Geophys. Res. Lett, in press.

Seneviratne, S.I., et al. 2010, in prep. (CECILIA special issue): Climate change and extreme events in Central and Eastern Europe: The CECILIA statistical indices and extreme database

3.1.5. Other cited references

Koenker, R., 2005: *Quantile regression*, Cambridge University Press, New York, USA.

McKee, T. B., N. J. Doesken, and J. Kleist, 1993: The relationship of drought frequency and duration to time scales, Eighth Conference on Applied Climatology, Anaheim, California, USA.

Seneviratne, S. I., D. Lüthi, M. Litschi, and C. Schär, 2006: Land-atmosphere coupling and climate change in Europe, *Nature*, 443 (7108), 205–209.

Teuling, A. J., M. Hirschi, A. Ohmura, M. Wild, M. Reichstein, P. Ciais, N. Buchmann, C. Ammann, L. Montagnani, A. D. Richardson, G. Wohlfahrt, and S. I. Seneviratne, 2009: A regional perspective on trends in continental evaporation, *Geophysical Research Letters*, 36 (L02404), doi:10.1029/2008GL036,584.212

3.2. DMI

DMI significantly contributed to the development of the CECILIA extreme database, which it is hosting (Section 2). Furthermore, it was also responsible for deliverable D4.2.

In addition, DMI is currently preparing a publication for the CECILIA special issue, which focuses on the added value of the high-resolution simulations (Christensen et al. 2010, in prep.). In the following figures we compare average precipitation, and a couple of summer wet-day precipitation percentile ratios: (p(70)-p(30)/p(50) and p(99)/p(50)). The first of these two is a dimensionless measure of the width of the central part of the precipitation intensity spectrum; the latter is a measure of the tail. These quantities can all be calculated on the basis of the CECILIA WP4 extremes indices.

The high-resolution simulation seems to have problems with the overall precipitation amounts, which are too high. Conversely, the percentile ratios are smaller than for the driving simulation in spite of the expectation of higher extremes with higher model resolution. This indicates that the high-resolution spectrum is not just a scaled version of the lower-resolution spectrum, but rather that the spectrum has somehow been shifted towards higher values. Further analyses should clarify this deviation.

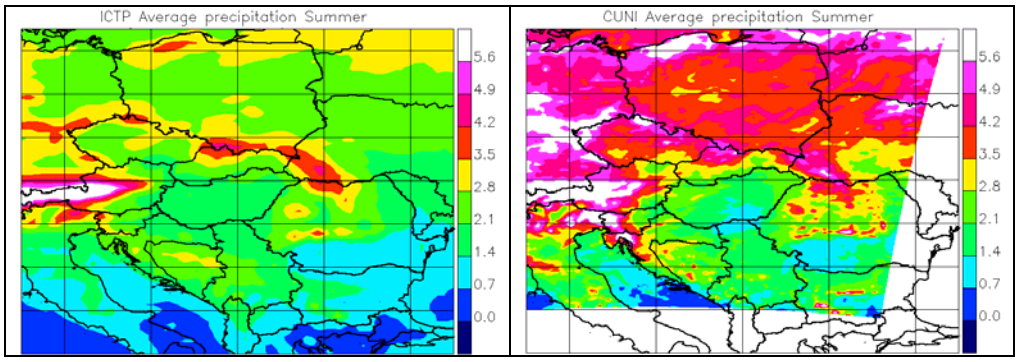

Figure 3.2.1. *Average precipitation over Central/Eastern Europe in mm/day for summer. Panels: ICTP/ECHAM5 25-km driving simulation 1961-1990; CUNI 10-km downscaling of ICTP/ECHAM.*

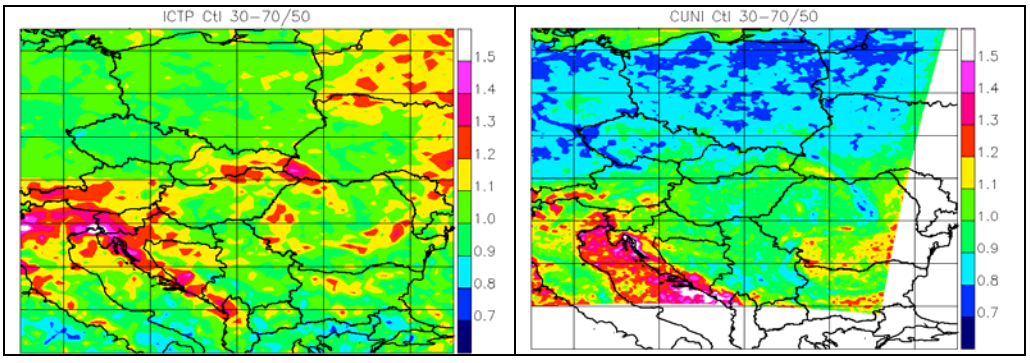

Figure 3.2.2. *Difference between 70th and 30th percentiles divided by the median for summer.*

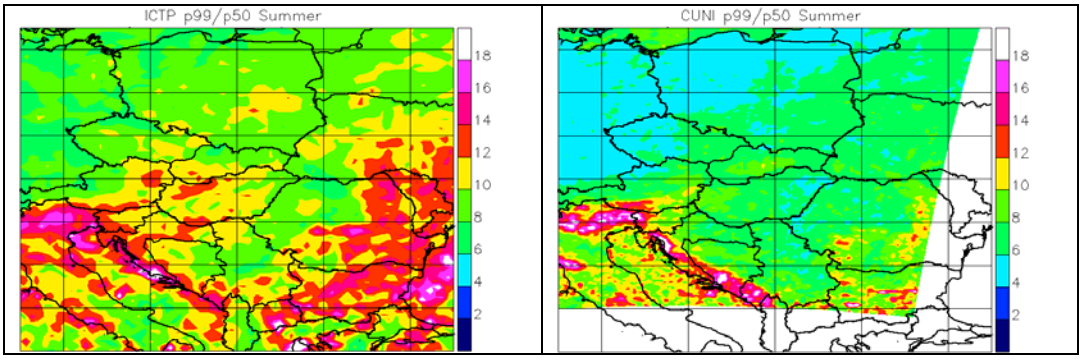

Figure 3.2.3. *99th percentile divided by median for summer.*

3.3. CHMI

As part of WP4, CHMI focused both on methodological aspect of extreme indices processing and carrying out calculations for the area of the Czech Republic. Many of the tasks were done in cooperation with IAP.

For the calculation of WP4 indices, the software ProClimDB developed by Petr Štěpánek was prepared and used, as one of the three possibilities (softwares) available within WP4 (see Section 2). This windows application is user friendly but is not as efficient for large datasets calculation as Matlab codes of Fredric Boberg (DMI) and the source code is not available (compared to R scripts of Martin Hirschi, ETH). On the other hand ProClimDB software includes tools for quality control, homogenization and many other possibilities.

Before the calculation of indices, the station data were subjected of thorough quality control and homogenization using the AnClim and ProClimDB software (Štěpánek, 2008). Details about the process can be found e.g. in Štěpánek *et al.* (2009). After detection and correction of outliers and time series homogenization, the gaps in the station data were filled using neighboring stations (applying geostatistical techniques). The so-called technical series were created for various meteorological elements for the area of the Czech and Slovak Republics and the northern part of Austria. For the indices calculation and the area of the Czech Republic itself, technical series of 268 climatological stations were available.

The 268 station positions with technical series were also recalculated (interpolated) into the ALADIN-Climate/CZ grid of 10 km horizontal resolution. Correction of ALADIN-Climate/CZ outputs (RCM driven by GCM ARPEGE with the IPCC A1B emission scenario) has been carried out for the area of the whole Czech and Slovak Republics, for both time slices, near (2021-2050) and further future (2071-2100) (details about methodology can be found in Deliverable D3.1). Results of indices calculation were then compared using original (biased) and corrected RCM outputs (done in cooperation with IAP). In the same way, also correction and comparison for RegCM has been processed.

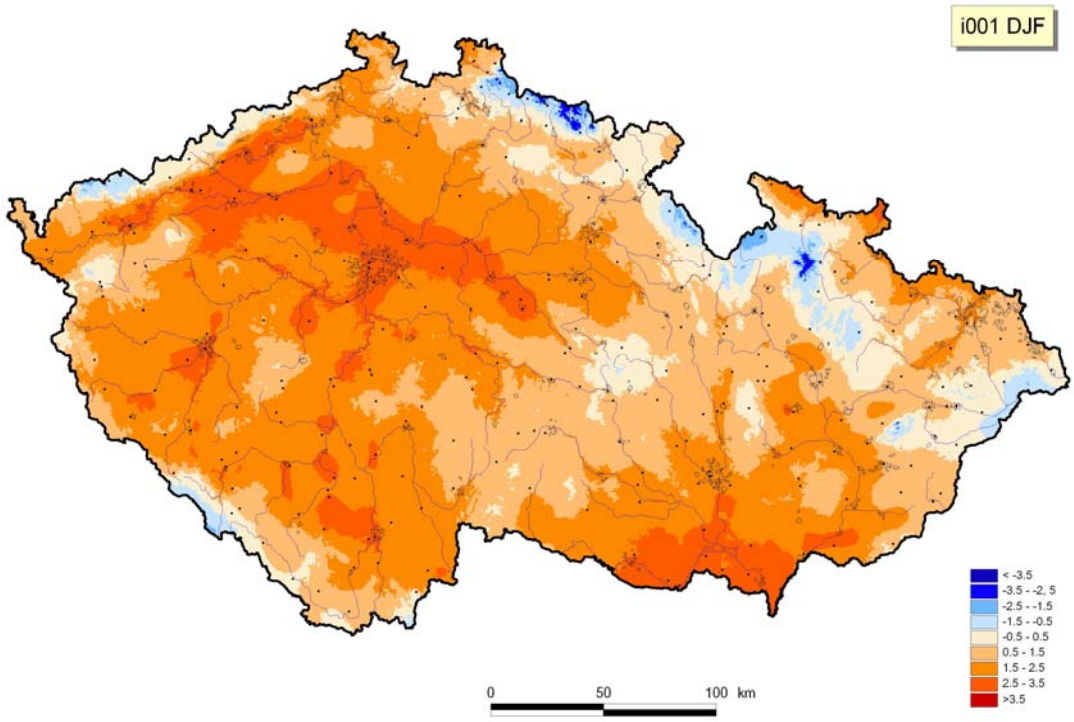

Fig. 3.3.1. Maximum temperature [°C] for the area of the Czech Republic from outputs of ALADIN-Climate/CZ (driven by GCM ARPEGE) in the period 1961-1990. DJF

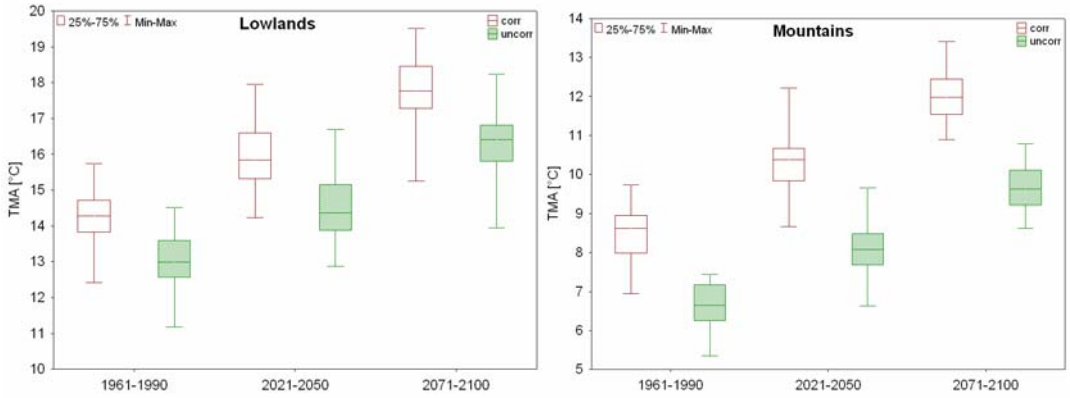

Fig. 3.3.2. Corrected and uncorrected maximum temperature [°C] for Czech and Slovak lowland (left) and mountainous regions (right) in the periods 1961-1990, 2021-2050 and 2071-2100

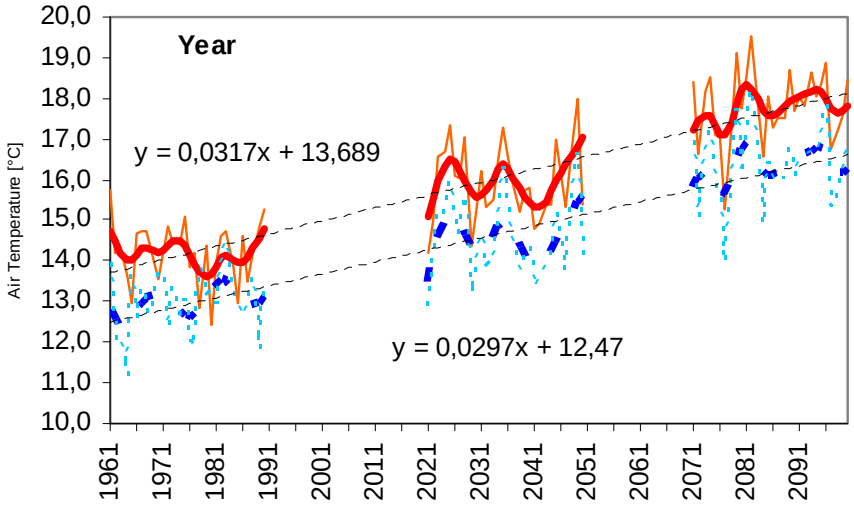

Fig. 3.3.3. Corrected and uncorrected maximum temperature [°C] for Czech and Slovak lowland regions in the periods 1961-2100 (solid line – corrected model outputs; dashed line uncorrected outputs)

References and relevant publications

Štěpánek, P., 2008: ProClimDB – software for processing climatological datasets. CHMI, regional office Brno. http://www.climahom.eu/ProcData.html.

Štěpánek, P., Skalák, P. and Farda, A., 2008: RCM ALADIN-Climate/CZ simulation of 2020-2050 climate over the Czech Republic. In: Rožnovský, J., Litschmann, T. (eds): Bioklimatologické aspekty hodnocení procesů v krajině (Mikulov 9. – 11.9.2008). CD-ROM. ISBN 978-80-86690-55-1

Štěpánek, P., Farda, A. and Skalák P., 2009: Czech and Slovak Republic according to RCM ALADIN-Climate/CZ outputs in the periods 2021-2050 and 2071-2100. In: Pribullova, A., Bicarova, S. (eds.), Sustainable Development and Bioclimate - Reviewed Conference Proceedings. Geophysical Institute of the Slowak Academy of Sciences and Slovak Bioclimatological Society of the Slovak Academy of Sciences., Stara Lesna, 2009, pp 58-59. ; ISBN: 978-80900450-1-9

Štěpánek, P., Zahradníček, P., and Skalák, P., 2009: Data quality control and homogenization of air temperature and precipitation series in the area of the Czech Republic in the period 1961–2007. Advances in Science and Research, 3, 23–26, 2009 http://www.adv-sci-res.net/3/23/2009/

3.4. NMA

NMA was involved in all WP4 deliverable and led the deliverable D4.4. The main results can be summarized as follows:

3.4.1 Observed extreme indices

- The extreme indices (EI) for 162 Romanian stations available for the period 1961-1990 has been calculated after the quality control of the daily data contributing to D4.2.
- Exemplification with the some indices for two selected seasons, winter (DJF) and summer (JJA), and annual (ANN) shows that the spatial distribution of EIs for the period 1961-1990 both at seasonal and annual time resolution reflects the climate characteristics of Romania that is influenced by its orography.
- Both mean Tmax (I001) and mean Tmin (I002) show highest values in the southern part of Romania, mostly enhanced during summer, being in agreement with spatial distribution of Tmean (I003) (not shown).
- The highest percentage of summer days (I058) and tropical nights (I059) (not shown) have been identified in the southern part of the country as well as for hot days (I066) and extremely hot days (I067)
- The highest percentage of severe cold days (I068) appears in the Carpathians and adjacent areas (not shown).

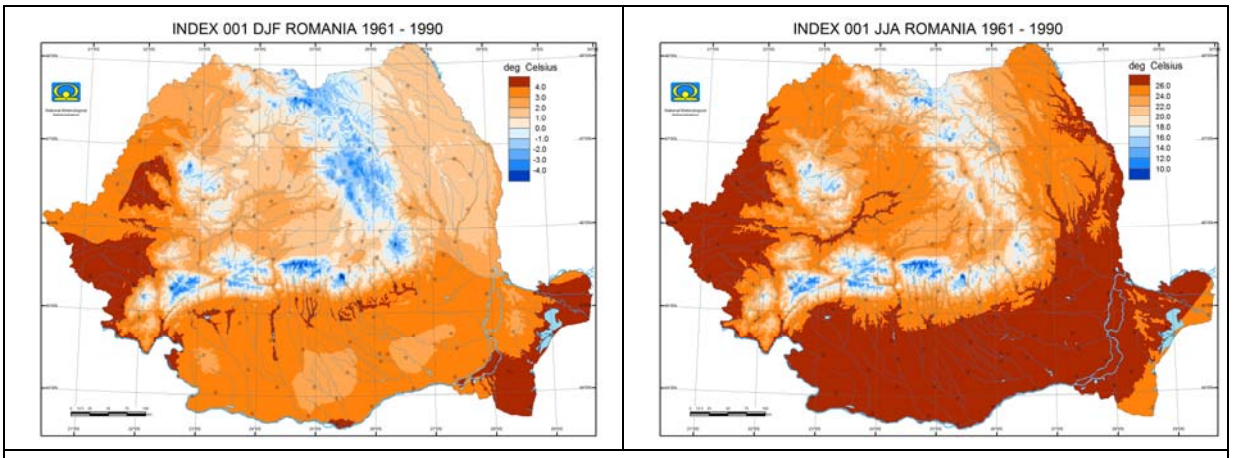

Index 001 - Mean Tmax – daily max averaged over 1961-1990

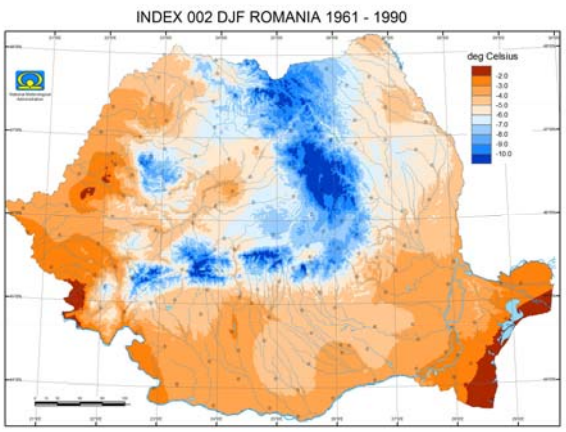

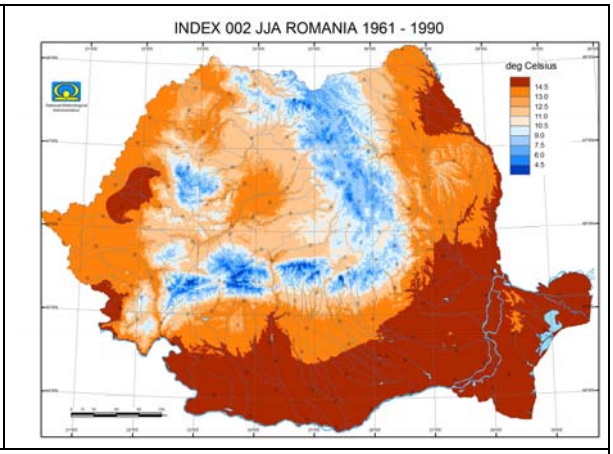

Index 002 - Mean Tmin - daily min averaged over 1961-1990

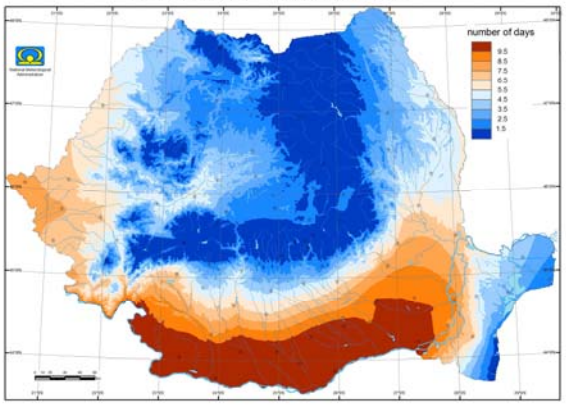

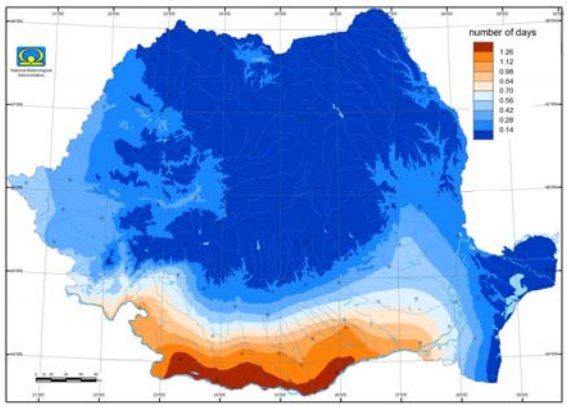

a) Index 066 - Percentage of hot days - %age of days with Tmax ≥ 30C
b) Index 067 - Percentage of extremely hot days - %age of days with Tmax ≥ 35C

3.4.2 Observed and projected links between extreme precipitation in Romania and large scale circulation

The results related to the link between regional-scale heavy precipitation in Romania and the large-scale circulation patterns using observational data have been reported to the deliverable D4.3. The nonhierarchical *K*-means clustering was used to classify the large scale mean sea level pressure associated to heavy precipitation days in the intra-Carpathian region in Romania during all seasons for the period 1961-2006.

The summary results shown that

- The large scale patterns associated to precipitation exceeding the selected thresholds are similar for all seasons.
- The distribution of the days exceeding the precipitation thresholds into clusters is uneven during the seasons and points out for the prevailing flows : zonal, high latitude zonal, SW and SE (European blocking).

Zonal circulation

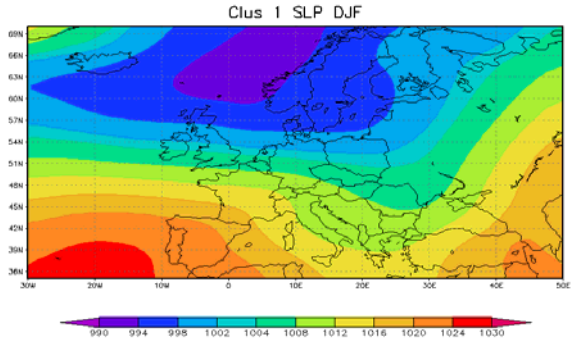

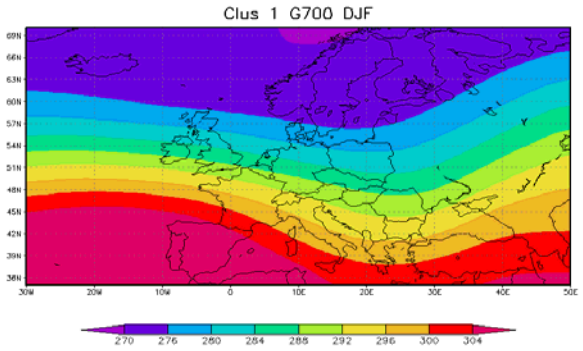

NW circulation

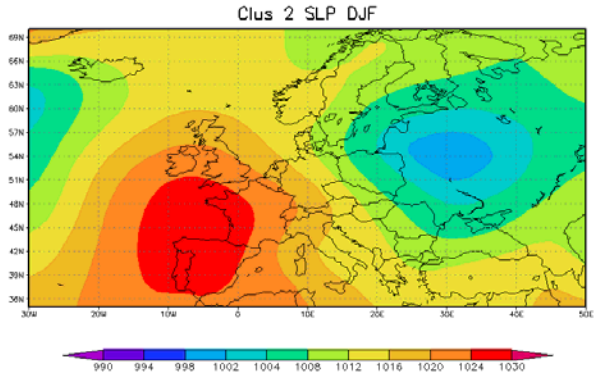

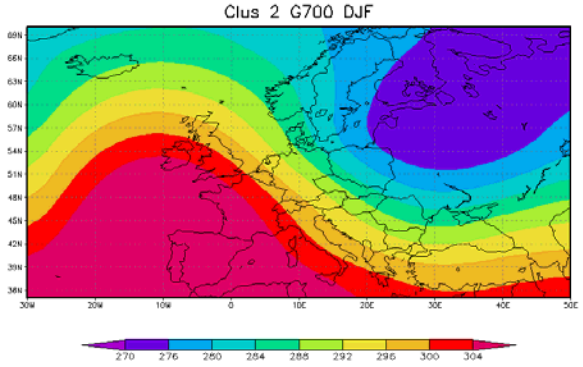

High latitude zonal circulation

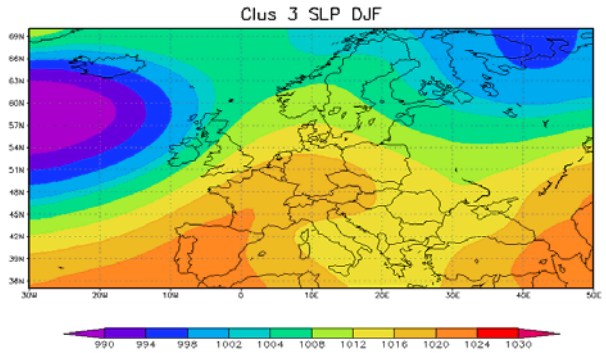

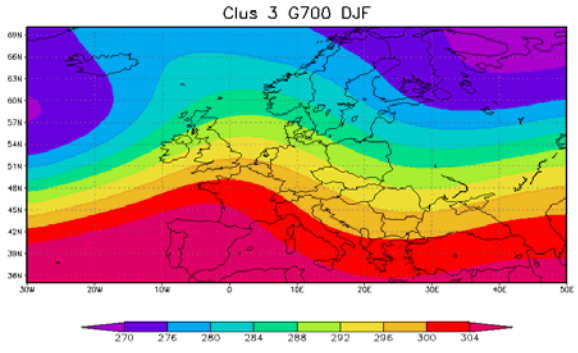

SW circulation

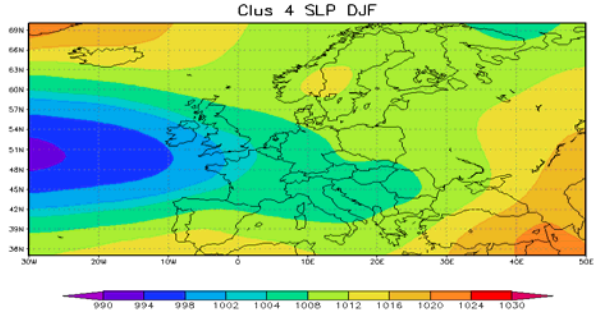

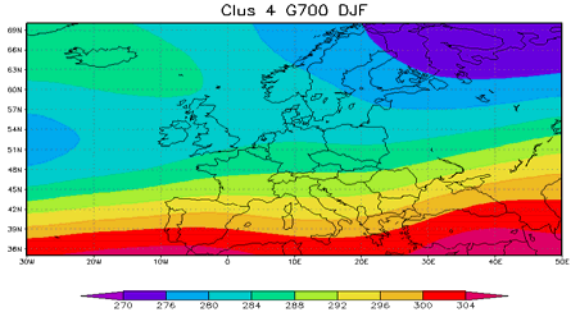

E circulation

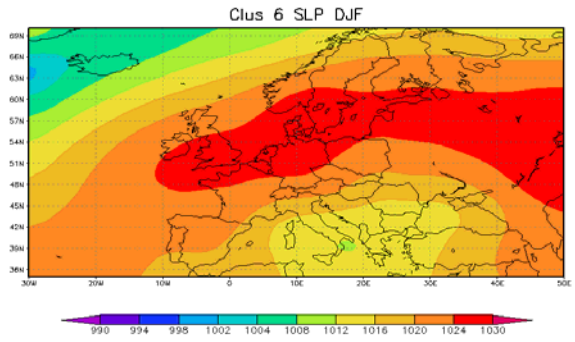

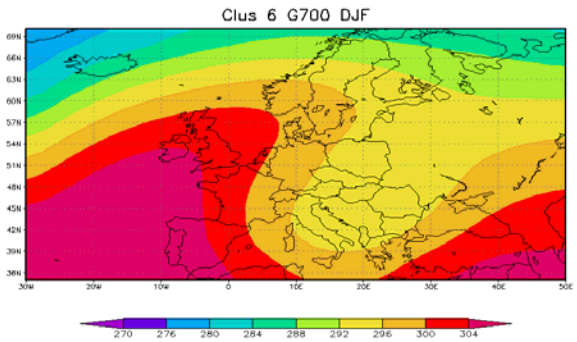

SE circulation (European blocking)

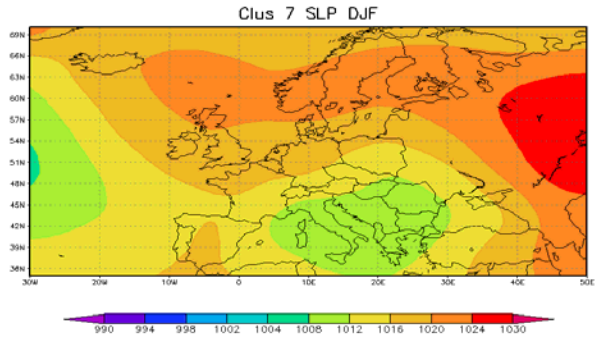

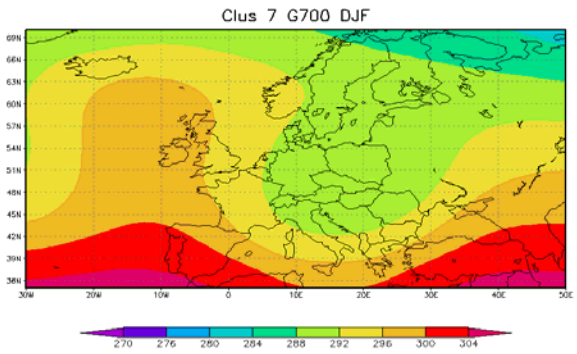

The circulation patterns for SLP (left panels) and the corresponding z700 hPa (right panels) associated to heavy precipitation in the intra-Carpathian region of Romania

A paper highlighting the changes in circulation patterns associated to extreme precipitation in Romania based on the extreme precipitation indices calculated for simulation data with the RegCM at 10 km and the large scale mean sea level pressure and geopotential high at 500 hPa from the coupling model at 25 km is in preparation (see 3.4.5).

3.4.3 Changes in extremes indices of temperature and precipitation

The results related to the projected changes in the selected indices out of 131 calculated for temperature and precipitation data simulated at 10 km over Romania domain been reported to the deliverable D4.4 led by NMA.

Temperature related extreme indices

- Simulated winter and summer daily maximum temperature are projected to increase by both time slices (2021-2050, 2071-2100) relative to the reference period (1961-1990). In Romania the projected changes in winter are about 2-2.4 °C in the eastern part of the country and over the Black Sea by the middle of the 21st century and about 3.4-4.2 °C by the end of the 21st century. During summer, the projected changes are more enhanced over the southern part of the country ranging 0.5 to 0.8°C by the mid 21st century and 3.4 to4.3°C by the end of the 21st century.

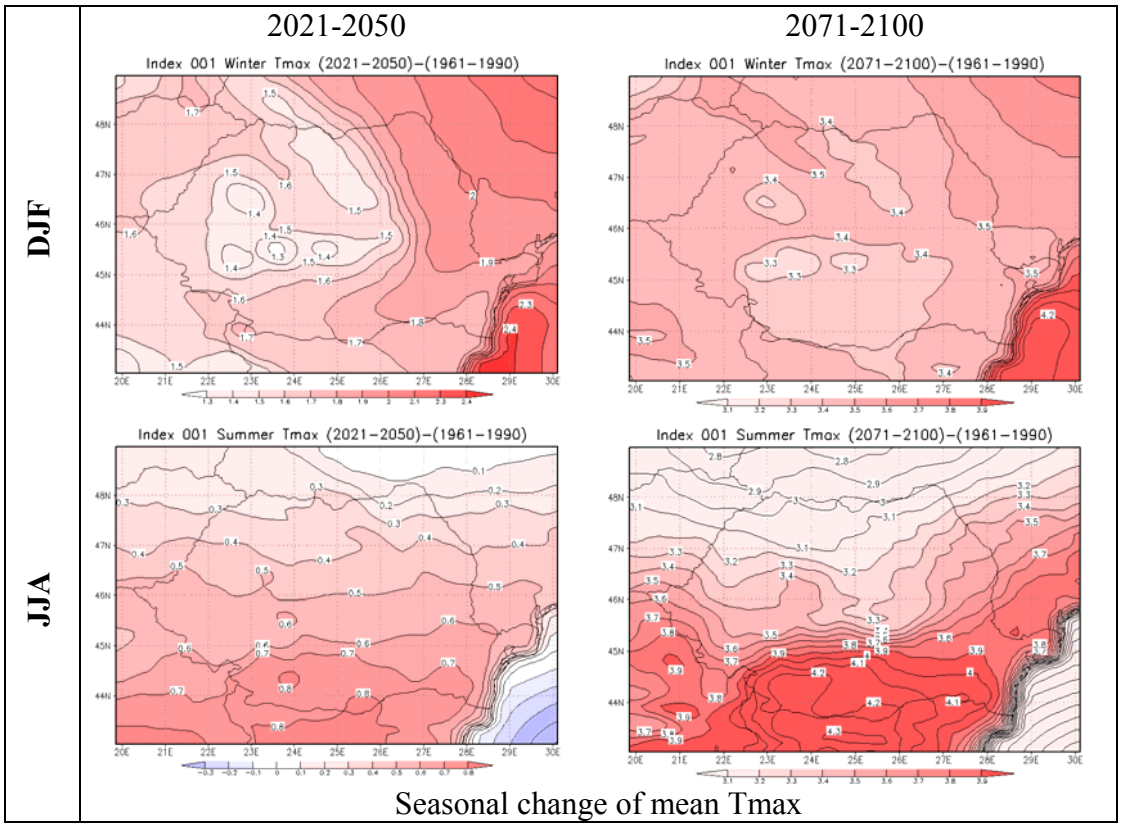

Seasonal change of mean Tmax

- Similarly to the daily maximum temperature, simulated winter and summer daily minimum temperature are projected to increase by both time slices (2021-2050, 2071-2100) relative to the reference period (1961-1990). Also, similarly to the maximum temperature, the projected winter warming is larger than the summer warming for both periods (1.6°C to 2.3 °C in the eastern part of the country and over the Black Sea by mid 21st century and, about 3.4°C over the northern half of the country and 4.2 ºC over the Black Sea by the end of the 21st century.

During summer the projected changes are expected to be larger in the southern half of the country ranging between 0.6 to 0.8°C by the mid 21st century and between 3.4°C and 4.1°C by the end of 21st century.

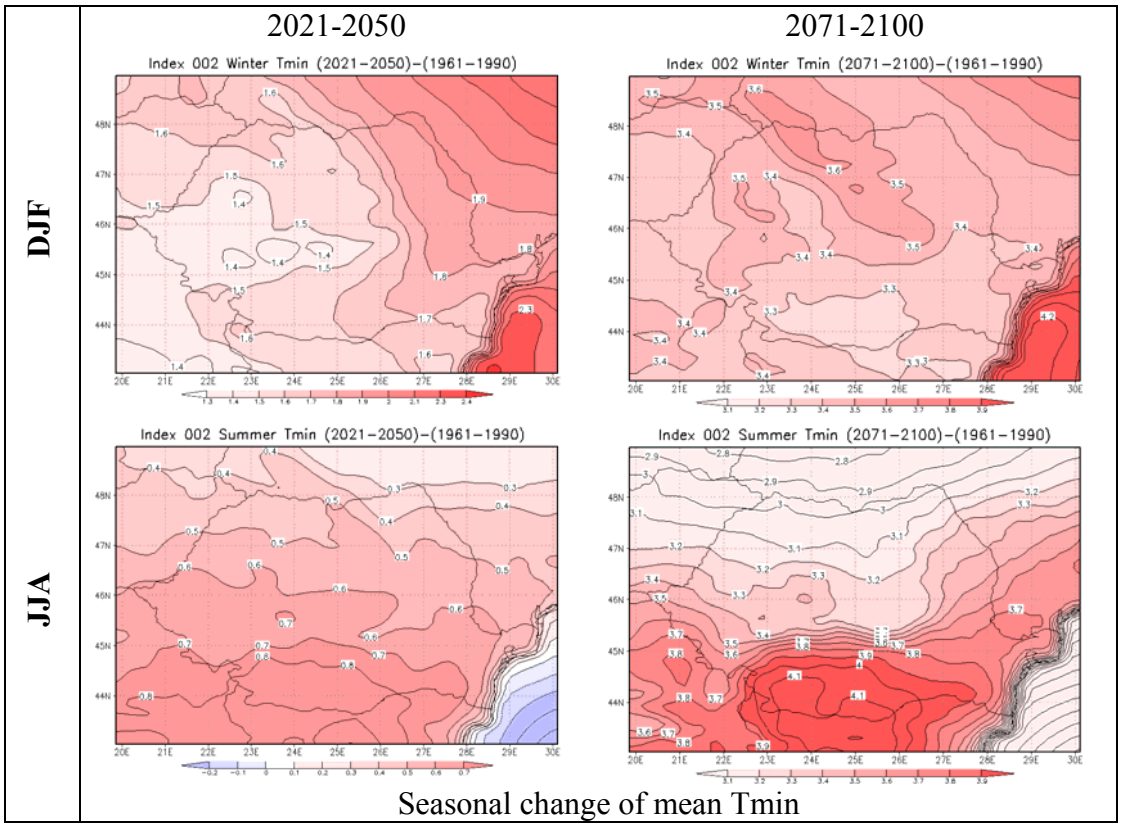

Seasonal change of mean Tmin

- Hot days (when the Tmax is larger than 30 °C) occur mainly in June-August but they can occur in May and September in Romania.
Comparing to the reference period and increase of the percentage of hot days up to 7% of the total days are expected by the middle of the 21st century and up to 40% by the end of the 21st century , in the southern part of the country.

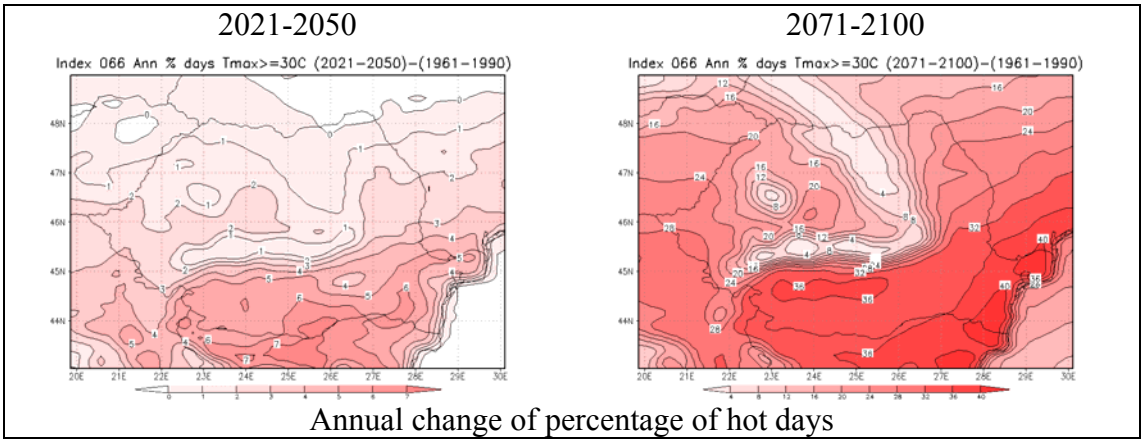

Annual change of percentage of hot days

Precipitation related extreme indices
- In general, simulated winter daily mean precipitation is projected to increase in Romania in the north-western part of the country and at high altitudes during both periods. By the middle of the 21st century the daily mean precipitation is expected to

slightly decease mostly in the south-eastern part of the country while by the end of the century the decrease in daily mean precipitation is expected to be enhanced up to -0.9 mm/day as compared to the reference period. The climate is likely to become wetter in the north-western part of the country in winter and drier over most of the territory but more enhanced in the north western part of the country and at high altitudes.

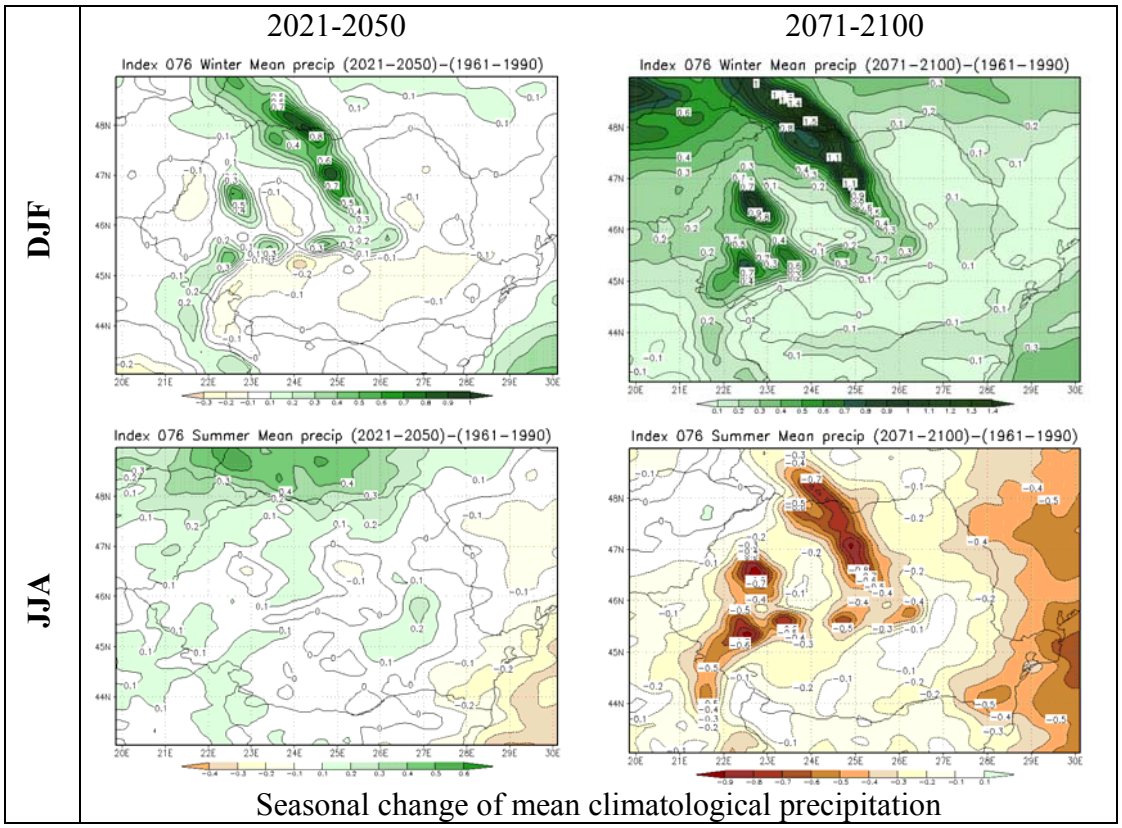

Seasonal change of mean climatological precipitation

- The percentage of wet days during winter is projected to decrease in the extra Carpathian regions up to -3% being more enhanced in the south-western part of the country. In the north-western part of the country the percentage of wet days will increase as compared to the reference period 196-1990 up to 5% by middle 21st century and up to 3% by the end of the century.
During summer, the percentage of wet days will decrease all over the country up to -2%, excepting a small area in the north-western part of the country where it will increase up to 3% by mid of the 21st century. The decrease of the percentage of wet days is expected over the whole territory of Romania by the end of the century, being more enhanced in the western and south western part of the country up to -8%

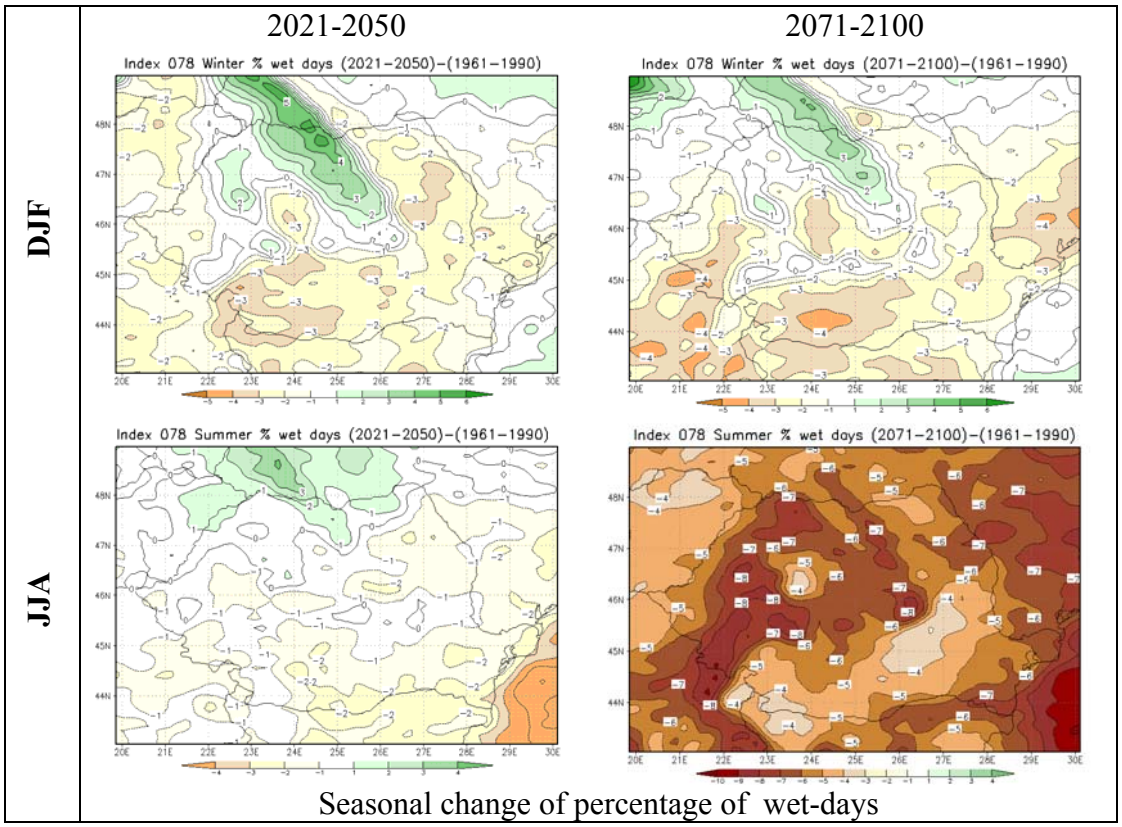

Seasonal change of percentage of wet-days

- During winter the simulated greatest 1-day total rainfall is projected to slightly decrease locally in the western and eastern part of the country and to increase with up to6 mm/day in the mountains and the central plateau by the middle of 21st century. By the end of the century the simulated greatest 1-day total rainfall is projected to increase all over the country during winter with an average of 4 mm/day both intra and extra Carpathians while at high altitudes this index will increase with up to 16 mm/day.

During summer the greatest 1-day total rainfall is projected to increase up to 8 mm/day in the extra Carpathians and central plateau and to decrease in the eastern part of the country along the western coast of the Black Sea and adjacent regions by the middle of 21st century. Similar patterns of changes are projected in summer by the end of the century when the increase of this index is expected with up to 12 mm/day and the decrease of this index up to 12 mm/day.

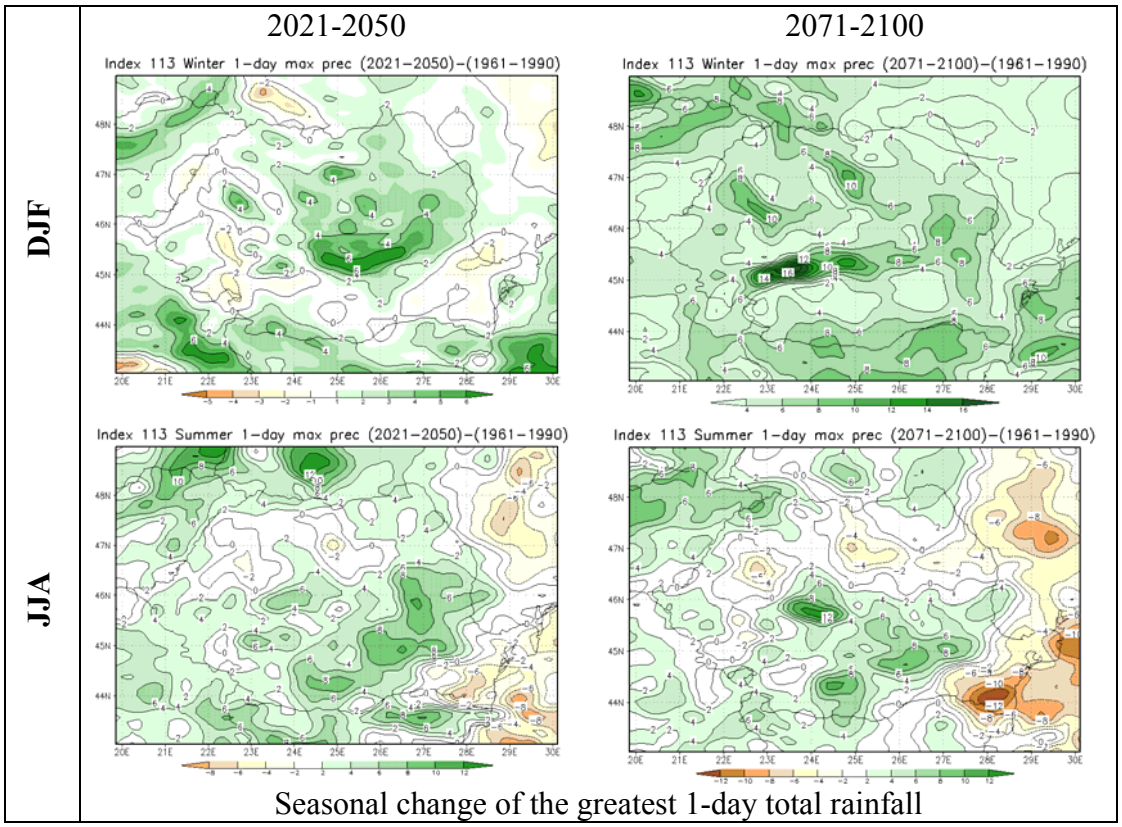

Seasonal change of the greatest 1-day total rainfall

A paper presenting the oobserved and projected climatic extremes over Romania is in preparation (see 3.4.5)

3.4.4 Impact of soil moisture on extremes in Romania

The role of soil moisture for extremes in regional climate simulations over Romania domain were investigated as part of deliverable D4.5. For details, please refer to the report on deliverable D4.5.

For the Romania region, sensitivity experiments with fix/variable soil moisture content for actual climate (1961-1990) and future climate (2071-2100) sustained the idea that the entire change in temperature variability is explained by the land-atmosphere coupling. These also confirmed the results obtained through similar but at coarser resolution experiments done at ICPT: the change in resolution doesn't change the results already obtained in the 25 km simulation.

Preliminary results obtained during sensitivity experiments over Romania are presented below.
A paper to highlight the impact of soil moisture on climate extremes over Romania is in preparation (see 3.4.5)

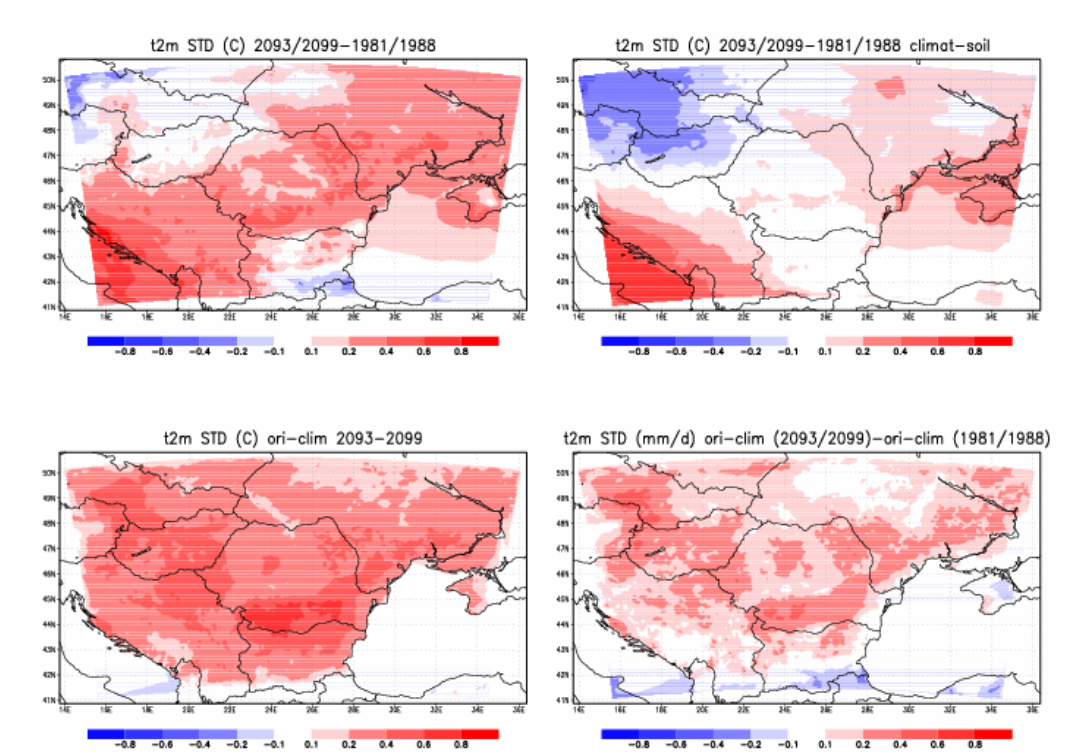

Changes in temperature standard deviation for the far future coupled simulation (top left column) and changes for the same period for the uncoupled simulation (top right column). Difference for the far future coupled and uncoupled temperature variability (bottom left panel) and difference between the far future temperature variability coupled and uncoupled change (bottom right panel)

3.4.5 List of publications in preparation for peer-reviewed journals

Boroneant,C, Boberg, F., Caian, M., Dumitrescu, A.: (in prep) Observed and projected climatic extremes over Romania

Boroneant, C., Caian, M. Esteban, P.,: (in prep) Changes in atmospheric circulation patterns producing extreme precipitation in Romania

Caian, M., Boroneant, C., Coppola E., (in prep) : Impact of soil moisture on climate extremes over Romania; Sensitivity experiment

3.5. CUNI

In addition to the application of the RegCM for regional climate change scenario construction as a basis for the CECILIA Project experiments have been performed in connection to the activities of WP2 dealing with further model development (D2.7) as well as for the WP4 where sensitivity of the models and some processes under the

climate change was studied (D4.5). As in RegCM application at CUNI, despite of the precipitation bias partly removed by modification done under cooperation of ELU and ICTP, the last decade simulation has shown that there is still significant bias during winter season, at CUNI further experiments were carried out trying to find possible further reduction of precipitation bias. We selected the parameter setting the relative humidity threshold of cloud formation as this was supposed to be sensitive to the resolution, moreover we tried to introduce the kind of s-shape function for this process representation. First experiment of the set was based on adjusting the internal parameters *rh0land* (increasing its value from 0.8 to 0.9) and *rh0oce* (increasing the value from 0.9 to 0.95) in RegCM „beta“ version, the second one described in this report used a modified function of fractional cloud coverage (s-shaped function) in RegCM „alfa“ version. The period simulated was 1961 and values were averaged over the inner part of the CUNI domain (i.e., without the buffer zone). The Fig. 3.5.1 shows that the parameter adjustment results in precipitation reduction, but despite of the expectation of the large scale precipitation impact mainly in spring and summer part of the year, in July the reduction occurs only in convective precipitation, while large-scale precipitation increases. Even in the summer months, the precipitation change is small (less than 10 %). Concerning the simple s-shape function choice shown in Fig. 3.5.2, the precipitation values decrease only in May, June and July and this is caused again by the decrease in convective precipitation. The differences are around or even more than 10 %, but not in the desired direction in the rest of the year (Fig. 3.5.3).

Comparing the two experiments, we see that the simple modification of fractional cloud cover parameters does not have the expected effect on precipitation. Although the modified parameters are connected rather with the large scale phenomena, both modifications end up affecting more the convection than large-scale precipitation. To get the intended bias reduction, further experiments and tests are planned together with more detailed analysis of the processes involved as well as radiation and cloudness outputs.

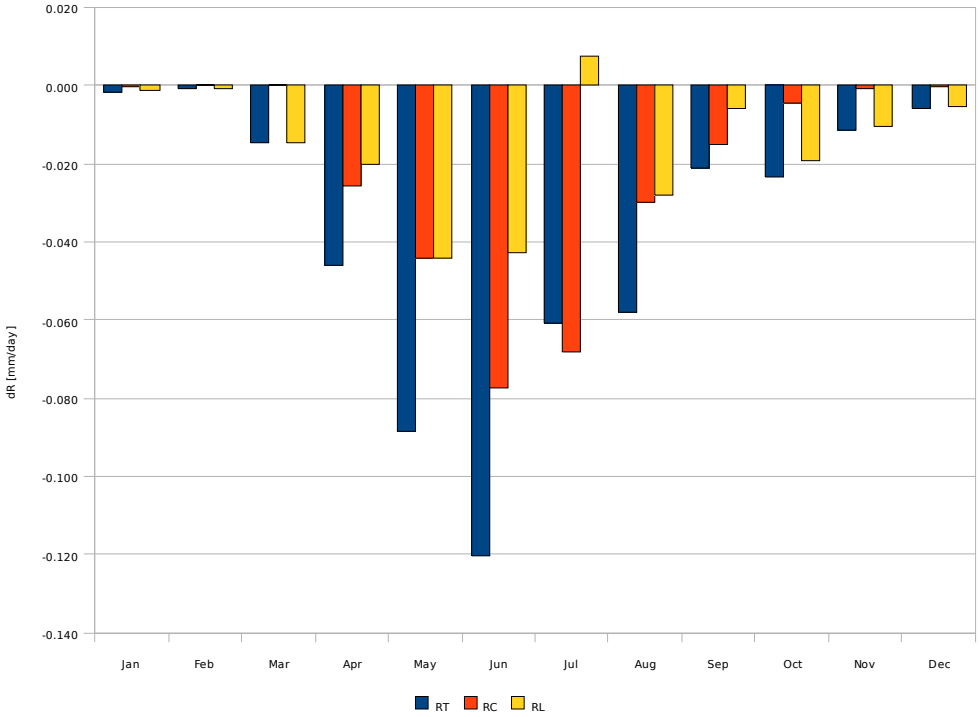

Figure 3.5.1: Precipitation change in adjusted model from original RegCM-beta, *rh0land* and *rh0oce* modified, RT = total precipitation, RC = convective precip., RL = large-scale precip.

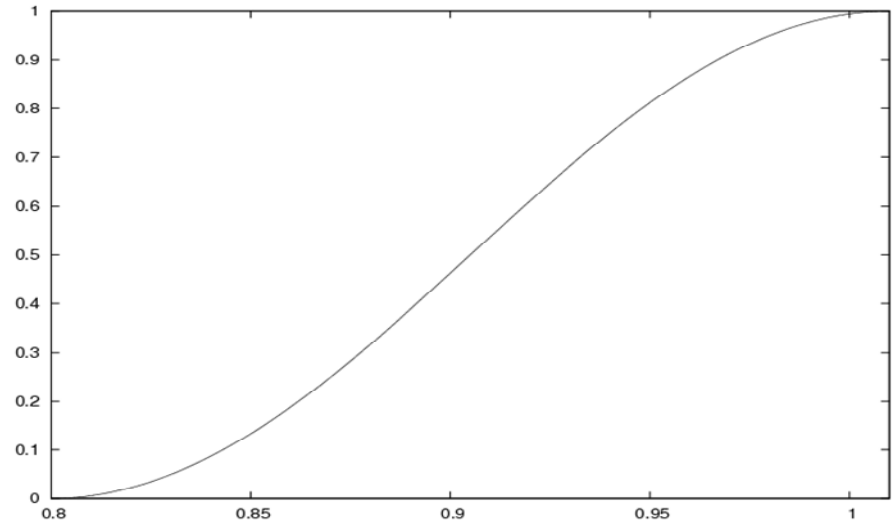

Figure 3.5.2: S-shaped function of fractional cloud coverage.

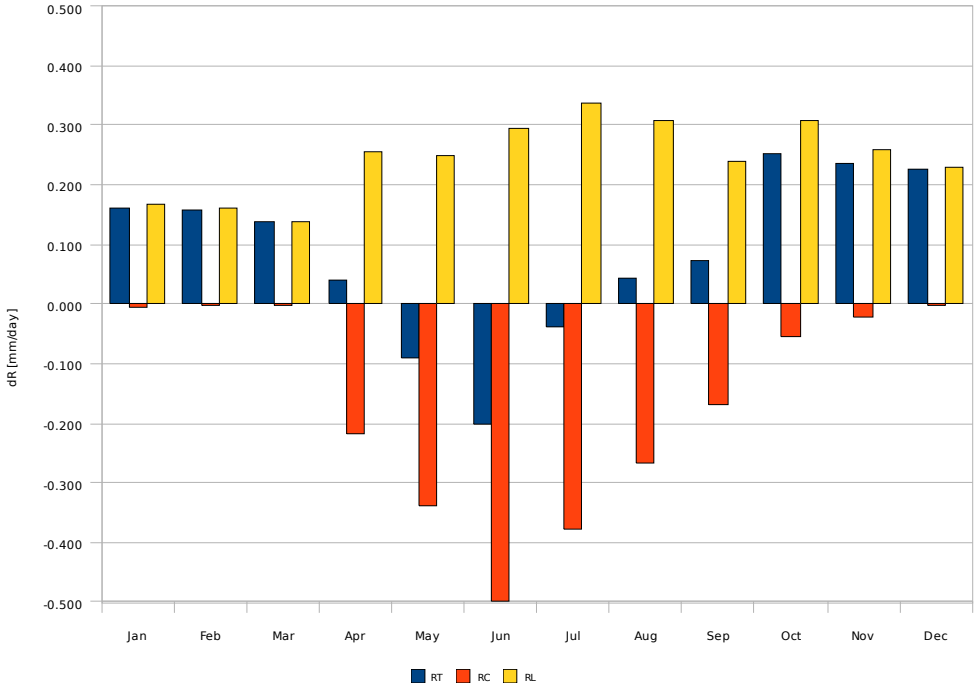

Figure 3.5.3: Precipitation difference between RegCM-alfa with original and modified fractional cloud coverage function.

3.6. ELU

ELU WP4 research resulted in several peer-reviewed journal papers and a book chapter. A list of these publications is provided in Section 3.6.3. Furthermore, research highlights regarding trend analyses of extreme climate conditions are provided in Sections 3.6.1 and 3.6.2.

3.6.1. Temperature indices

Simulated winter and summer daily maximum temperature are projected to increase by both future time slices relative to the reference period (1961-1990). In Hungary the projected changes are about 1 °C by the middle of the 21st century, and about 3 °C in winter and 4 °C in summer by the end of the 21st century. The projected winter warming is larger than the summer warming for the 2021-2050 period, while for the 2071-2100 it is smaller. The summer warming patterns in Hungary follow a zonal structure, the largest temperature increase is expected in the southern regions.

Summer days (when T_{max} is larger than 25 °C) may occur mainly in May-September in Hungary. In the reference period 6-20% of the total days are simulated as summer days, which means about 22-73 days in a year. Evidently, in the mountainous subregions (e.g., the Eastern Alps or the Carpathians), less summer days occur than in the lowlands of Hungary. By the near future (2021-2050) it is not likely to change too much in Hungary (the increase is only about 1-3%, which is not exceeding a week). However, by the end of the century (2071-2100) the annual percentage of summer days is likely to increase by about 7-14% in Hungary (left panel of Fig. 3.6.1). This implies that the

annual number of summer days is projected to exceed 110 days in a year in the southern part of the country, and may even reach as much as 120 days per year.

Hot days (when T_{max} is larger than 30 °C) may occur mainly in June-August in Hungary. In the reference period less than 8% of the total days are simulated within the country as hot days, which means less than 30 days/year on average. Similarly to the percentage of summer days, the simulated changes by 2071-2100 in Hungary are much larger than the changes by 2021-2050 (4-12% and 1-3%, respectively). Also similarly to the summer days, the large frequency changes are projected to occur in the southern part of the country (right panel of Fig. 3.6.1) where according to the RegCM simulations about 62 days will be considered hot days yearly.

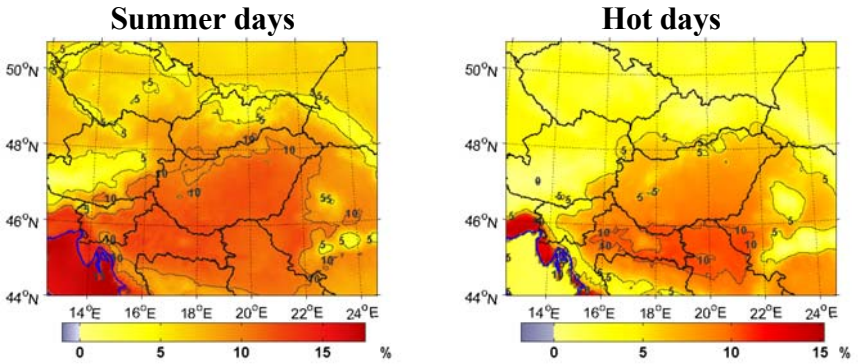

Fig. 3.6.1: Projected mean change of annual percentage of summer and hot days by 2071-2100 (reference period: 1961-1990)

Unlike the previous temperature parameters related to warm conditions, the occurrence of frost days (when T_{min} < 0 °C) is mainly in the winter half-year. According to the RegCM climate simulations 55-128 days can be considered as frost days in Hungary in the reference period (1961-1990): in the lowlands (below 200 m above the sea level) less than 70 days/year, in the higher elevated subregions (i.e., the northern/northeastern part of the country) frost days are more frequent, exceeding 100 days/year. In the future, the frequency of frost days is likely to decrease, by about 3-8% and 8-14% in Hungary by 2021-2050 and 2071-2100, respectively (Fig. 3.6.2). Thus, by the end of the 21st century, the annual number of frost days is projected not to exceed 55 days, and even smaller in the lowlands of the country, less than 25 days. The decrease is evidently larger in mountainous regions where frost days occurred more frequently in the past.

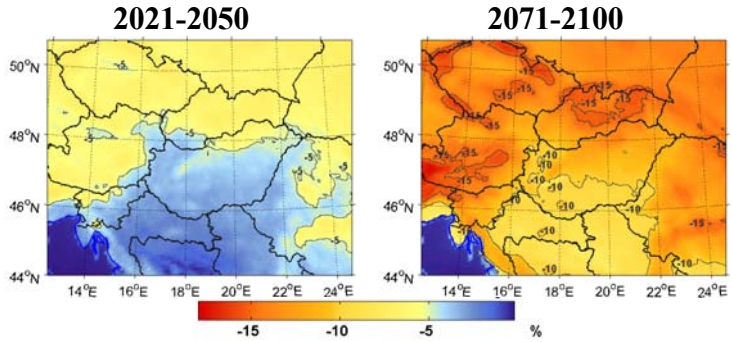

Fig. 3.6.2: Projected mean change of annual percentage of frost days by 2021-2050 and 2071-2100 (reference period: 1961-1990)

Among the temperature related extreme indices, one more example is selected, which has a strong influence on agriculture. Growing degree days (Fig. 3.6.3) are defined as the annual sum of the daily mean temperature values (T_{mean}) decreased by 4 °C when T_{mean} is larger than 4 °C. According to the simulated results, in the entire domain an evident increase of the growing degree days is expected for both future time slices compared to the reference period (1961-1990). Projected changes are larger for 2071-2100 than for 2021-2050 (in Hungary, the growing degree days are projected to increase by about 38% and 12% on average, respectively).

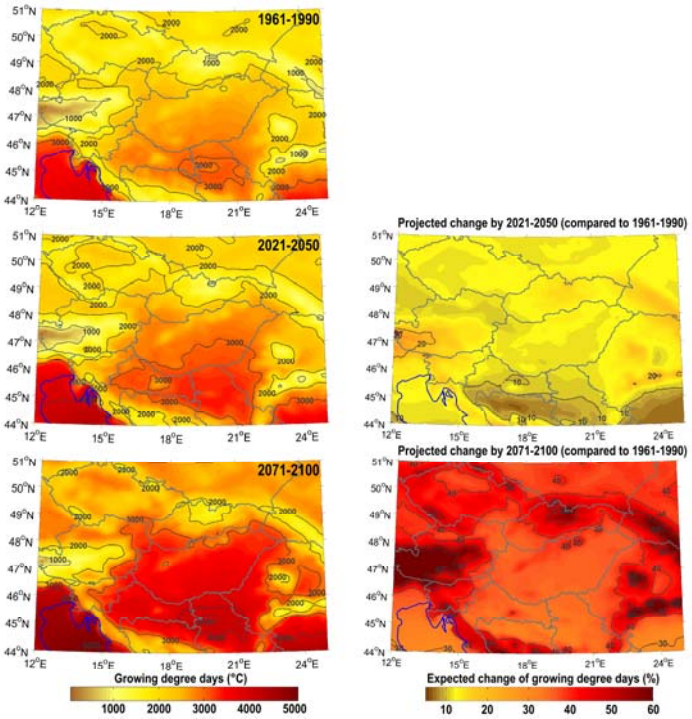

Fig. 3.6.3: Growing degree days (Sum of (T_{mean} – 4 °C) for all days with T_{mean} > 4 °C) based on simulated daily mean temperature

3.6.2. Precipitation indices

Simulated winter wet-day mean precipitation is projected mostly to decrease in eastern Hungary and increase in western Hungary by 2021-2050. In summer, large portion of the country (especially in east) may expect an increase of mean wet-day precipitation amount, decrease is projected only around the lake Balaton. The RegCM simulations show similar changing pattern by the end of the century for summer. In winter, the wet-day mean precipitation is projected to increase in the entire country (Table 3.6.1). The largest increase is about 30% in the northern mountainous region of Hungary.

Table 3.6.1: Projected mean seasonal change of wet-day precipitation for Hungary for 2021-2050 and 2071-2100 (reference period: 1961-1990)

Season	2021-2050	2071-2100
Winter (DJF)	(-0.5; +0.5) mm/day (-10%; +10%)	(0; 1.2) mm/day (0%; +20%)
Summer (JJA)	(-1; +1.2) mm/day (-10%; +22%)	(-0.5; +2) mm/day (-7%; +30%)

The percentage of wet days is projected to decrease for both winter and summer, and for both future time slices in Hungary. The simulated changes are larger by 2071-2100 than 2021-2050 (Fig. 3.6.4). The largest changes are projected for summer by the end of the 21st century, when the percentage is likely to decrease by as much as 10% in the country, which means about 9 days less wet day in a season (Table 3.6.2).

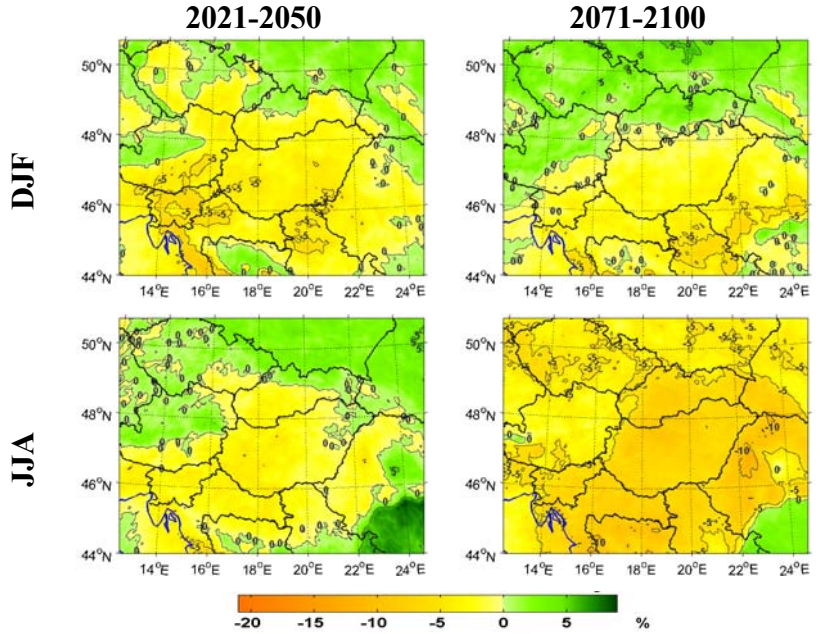

Fig. 3.6.4: Projected mean seasonal change of percentage of wet days (reference period: 1961-1990)

Table 3.6.2: Simulated mean seasonal percentage of wet days for Hungary for 1961-1990 (reference period), 2021-2050, and 2071-2100

Season	1961-1990	2021-2050	2071-2100
DJF ratio	25-43%	22-45%	25-45%
Simulated change	-	(-5%; 0%)	(-3%; 0%)
JJA ratio	25-40%	20-40%	15-30%
Simulated change	-	(-5%; +2%)	(-10%; -5%)

The simulated greatest 1-day total rainfall is projected to increase in Hungary by 2071-2100 in winter, the largest changes are expected in the northern mountainous region where it may increase as much as by 40% compared to the reference period (Fig. 3.6.5). Similar changes are projected in summer for the eastern part of the country, while for the western part the greatest 1-day total rainfall a decrease is expected on the base of the RegCM simulations. The seasonal mean daily maximum precipitation values determined from the RegCM outputs of the grid points located in Hungary for the three time slices and the corresponding projected changes relative to the reference period are shown in Table 3.6.3 for winter and summer.

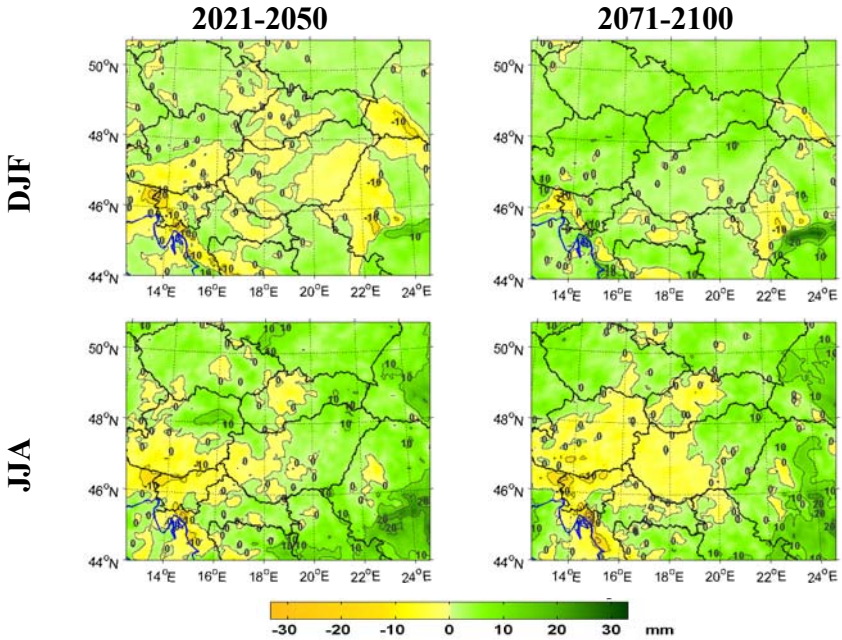

Fig. 3.6.5: Projected mean seasonal change of the greatest 1-day total rainfall (reference period: 1961-1990)

Table 3.6.3: The simulated mean seasonal greatest 1-day total rainfall for Hungary for 1961-1990 (reference period), 2021-2050, and 2071-2100

Season	1961-1990	2021-2050	2071-2100
DJF	15-30 mm	15-35 mm	18-40 mm
	-	(-5 mm; +5 mm)	(0 mm; +10 mm)
Simulated change		(-20%; +25%)	(0%; +40%)
JJA	20-30 mm	30-40 mm	20-30 mm
	-	(-5 mm; +10 mm)	(-5 mm; +10 mm)
Simulated change		(-20%; +50%)	(-25%; +50%)

Among the precipitation related extreme indices, one example is selected, which reflects the drought conditions. Annual maximum number of consecutive dry days are shown in Fig. 3.6.6 calculated from the simulated daily precipitation amount time series. The results suggest that in general, an increase is projected for the southern part of the domain, and a decrease for the northern part. Expected changes in absolute value are larger for 2071-2100 than for 2021-2050. In Hungary for both periods, consecutive dry days are projected to increase, thus, resulting in more severe drought, especially by the end of the 21st century (in some places the projected increase may exceed 5 days, which means 25% of the current climatic conditions).

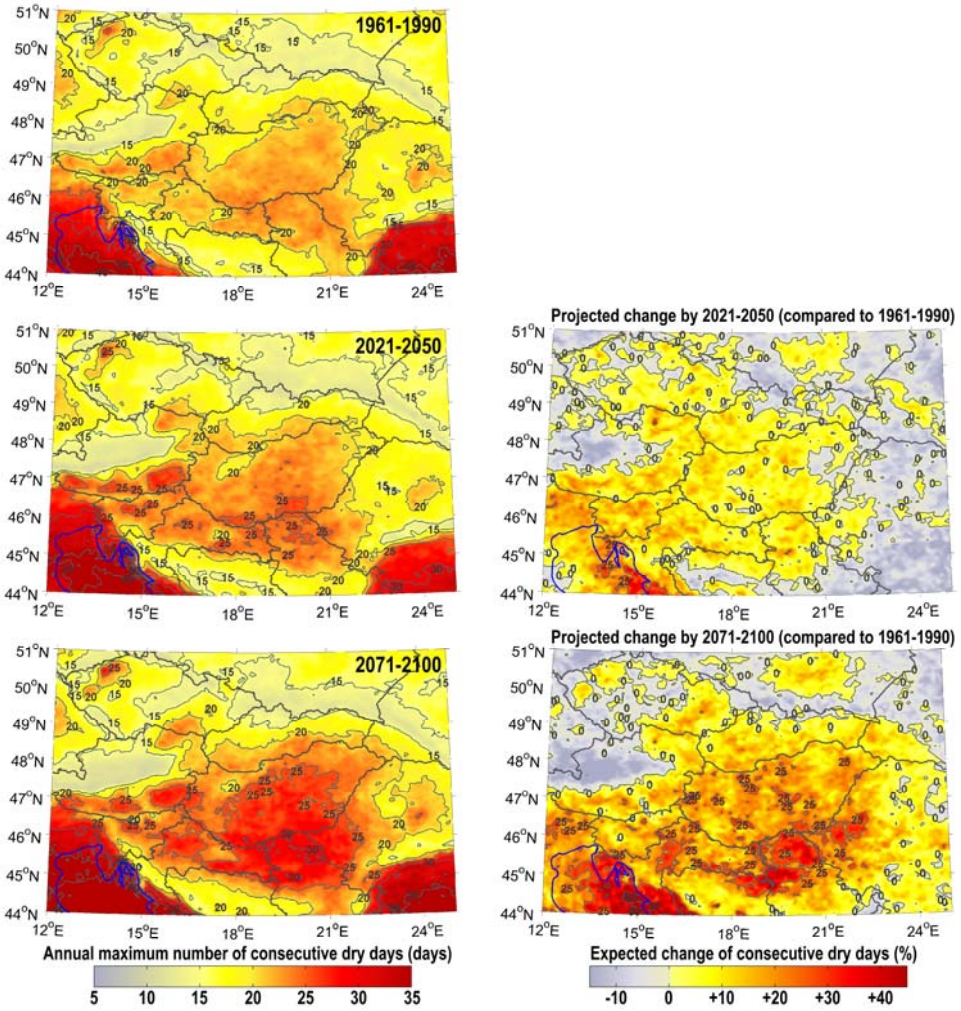

Fig. 3.6.6: Maximum number of consecutive dry days based on simulated daily precipitation amounts.

3.6.3. List of publications in peer-reviewed journals and book chapter

Bartholy J., Pongracz R., 2007: Regional analysis of extreme temperature and precipitation indices for the Carpathian Basin from 1946 to 2001. *Global and Planetary Change, 57, 83-95.* doi:10.1016/j.gloplacha.2006.11.002

Bartholy J., Pongrácz R., Gelybó Gy., Szabó P., 2007: Change of temperature extremes expected in the Carpathian basin by the end of the 21st century. *Klíma-21, 51, 3-17. (in Hungarian)*

Bartholy J., Pongrácz R., Gelybó Gy., Szabó P., 2008: What changes of the extreme climate conditions can be expected in the Carpathian basin by the end of the 21st century? *Légkör, 53/3, 19-23. (in Hungarian)*

Bartholy J., Pongracz R., Gelybó Gy., Szabó P., 2008: Analysis of expected climate change in the Carpathian basin using the PRUDENCE results. *Időjárás, 112, 249-264*.

Pongracz R., Bartholy J., Szabo P., Gelybo Gy., 2009: A comparison of observed trends and simulated changes in extreme climate indices in the Carpathian basin by the end of this century. *International Journal of Global Warming, 1, 336-355.* DOI: 10.1504/IJGW.2009.027097.

Pongrácz R., Bartholy J., Gelybó Gy., Szabó P., 2009: Detected and expected trends of extreme climate indices for the Carpathian basin. In: *Bioclimatology and Natural Hazards* (eds: Strelcova, K., et al.), pp. 15-28. Springer. DOI 10.1007/978-1-4020-8876-6_2.

3.7. IAP

IAP conducted analyses of extreme indices for the Czech republic in collaboration with CHMI (see Section 3.3.). In addition, it prepared another publication (Kysely and Beranova 2009), which is briefly summarized hereafter.

Summary

Observations as well as most climate model simulations are generally in accord with the hypothesis that the hydrologic cycle should intensify and become highly volatile with the greenhouse gas induced climate change, although uncertainties of these projections as well as the spatial and seasonal variability of the changes are much larger than for temperature extremes. In this study, we examine scenarios of changes in extreme precipitation events in 24 future climate runs of 10 regional climate models, focusing on a specific area of the Czech Republic (central Europe) where complex orography and an interaction of other factors governing the occurrence of heavy precipitation events result in patterns that cannot be captured by global models. The peaks-over-threshold analysis with increasing threshold censoring is applied to estimate multi-year return levels of daily rainfall amounts. Uncertainties in scenarios of changes for the late 21st century related to the inter-model and within-ensemble variability and the use of the SRES-A2 and SRES-B2 greenhouse gas emission scenarios are evaluated. The results show that heavy precipitation events are likely to increase in severity in winter and (with less agreement among models) also in summer. The inter-model and intra-model variability and related uncertainties in the pattern and magnitude of the change is large, but the scenarios tend to agree with precipitation trends recently observed in the area, which may strengthen their credibility. In most scenario runs, the projected change in extreme precipitation in summer is of the opposite sign than a change in mean seasonal totals, the latter pointing towards generally drier conditions in summer. A combination of enhanced heavy precipitation amounts and reduced water infiltration capabilities of a dry soil may severely increase peak river discharges and flood-related risks in this region.

Reference

Kyselý J., Beranová R., 2009: Climate change effects on extreme precipitation in central Europe: uncertainties of scenarios based on regional climate models. *Theoretical and Applied Climatology,* **95**, 361-374 [doi: 10.1007/s00704-008-0014-8].

3.8. OMSZ

Some WP4 research highlights from OMSZ are provided in Sections 3.8.1. and 3.8.2. A list of relevant publications is provided in Section 3.8.3.

3.8.1. Observed temperature trends in Hungary

Climate indices calculations require at least daily resolution of homogeneous time series without inhomogeneities, such as transfer of stations, changes in observation practice. It is a frequent occurrence that the sign of the slope implies a decreasing

trend on the data with artificial breaks, while the fitted trend to homogenized data implies an increasing tendency, or reverse. Interpolation of indices is not recommended directly for mapping procedures as the probability distribution functions are unknown of the several indices. Our suggestion is to interpolate the basic observations, namely daily maximum, daily minimum and daily average temperatures, and daily precipitation sums. The quality of gridded observations is strongly depends on the method what is used for this purpose. The whole period change of the Cecilia Index 66 (%age of days with daily maximum temperature ≥ 30°C) are shown in *Fig. 3.8.1*. The change arise by the point estimation of the linear trend and the changes according to the $\alpha = 0.1$ significance level confidence interval's lower bounder and upper bounder are indicated as well. Quality controlled, homogenized, completed and gridded observations were used for Cecilia indices calculations. The warming tendency is obvious in the region. The increasing of the rate of hot days is 11% at least, in areal average, but could exceed 35% from the mid 70's on the Great Plain, which is a natural handicaps part of the country.

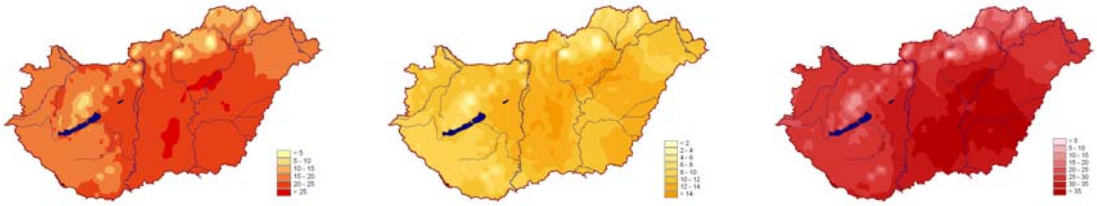

Figure 3.8.1 Observed changes of the Cecilia index 66 (%age of days with daily maximum temperature ≥ 30°C) in the period 1976-2007 in Hungary. The maps show the point estimated change (on the left), the change "at least" (in the middle) and "at the most" (on the right) on the α = 0.1 significance level

3.8.2. Future changes in Hungary

The daily temperature and precipitation indices resulting from Aladin-Climate simulations (AA) for two time slices: 2021-2050 and 2071-2100 versus control run forced by ERA40 (AE) were analysed for Hungary.

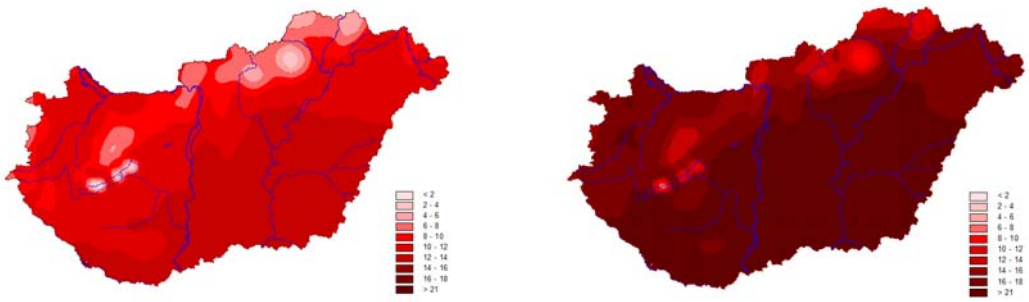

Figure 3.8.2 Cecilia index 066 %age of days with Tmax ≥ 30°C AA(2021-2050)-AE(1961-1990) and AA(2071-2100)-AE(1961-1990)

The rate of "hot days" (*Fig 3.8.2)* increasing is expected more than 10% in the period 2021-2050 on the Great Plain and it is more than 20% almost on the whole territory, excluding the mountainous area, in the period 2071-2100.

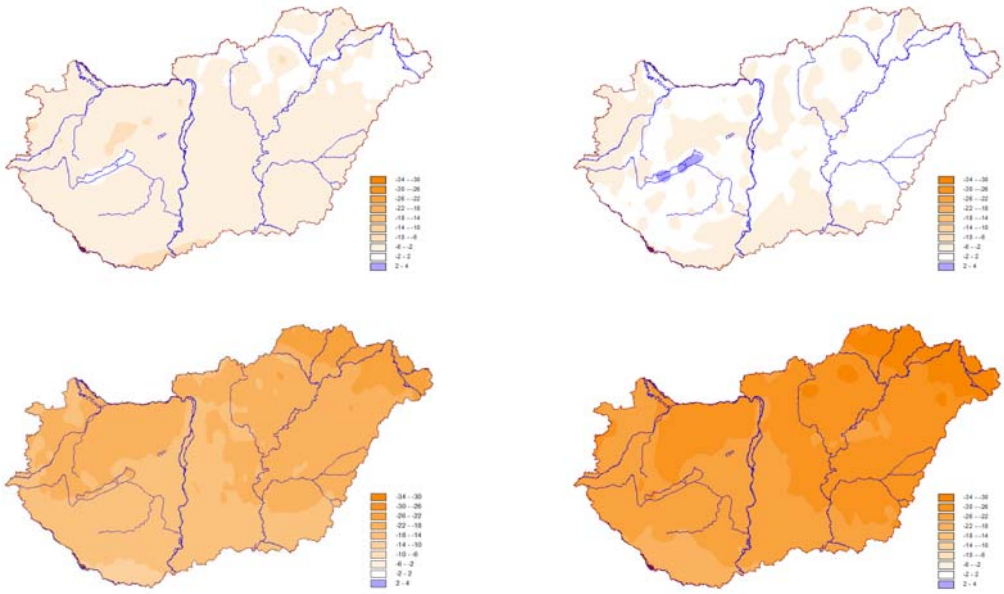

Figure 3.8.3.Cecilia index 078 Perc of wet days AA(2021-2050)-AE(1961-1990) and AA(2071-2100)-AE(1961-1990) for DJF on the top and for JJA at the bottom

Regarding the percentage of wet days (number of days where daily sum ≥ 1mm / total number of days) index (*Fig. 3.8.3*); there is an obvious decreasing in summer in projections versus the control run, especially in the 2071-2100 period. The order of negative change in the far future, in summer is larger, around -25% on the extended part of the country. The negative change in winter is approximately -15%, the spatial distribution shows a north eastern growth in both projection and season. These changes in the number of wet days pose a major challenge for agriculture in Hungary.

3.8.3. List of publications

Lakatos, M., Szentimrey, T., Bihari, Z., Szalai, S, 2008: Homogenization of daily data series for extreme climate indices calculation, Proceedings of COST-ES0601 (HOME) Action Management Committee and Working Groups and Sixth Seminar for Homogenization and Quality Control in Climatological Databases, Budapest, 2008. május 26-30.

Lakatos, M., Szentimrey, T., Bihari, Z., 2009: Gridded daily data series for mapping of extreme temperature and precipitation indices in Hungary, Proceedings of 2nd Conference on the Spatial Interpolation in Climatology and Meteorology, Budapest, 11-15 May 2009

Mika, J. and M. Lakatos, 2008: Extreme weather tendencies in Hungary: One empirical and two model approaches. In: Regional Climatic Change and its Impacts (J.Sigro, Brunet, M. and Aguillar E., eds.) Tarragona, 2008. Oct 8-11, 521-530 pp

3.9. ICTP

ICTP was responsible for deliverable D4.5. Please refer to the respective report for an overview of its WP4-related research highlights.

3.10. AUTH

AUTH contributed to deliverables D4.2 and D.4.3. The main related findings are summarized hereafter.

Large-scale circulation patterns, such as the ones connected to the North Atlantic Oscillation (NAO) or northern hemisphere atmospheric blocking, are known to control westerly flow of air into the European continent, thus affecting local weather and climate. Their effects on temperature and precipitation changes were investigated in detail over Europe using data from General Circulation Models (GCMs) and Regional Climate Models (RCMs) used as driving models in the framework of the project.

- NAO related effects
i) Past changes (1960-2000)
The analysis of both sets of data (GCM and CCM) shows a good agreement to the observed NAO effects over Europe, i.e. warm and wet over North-Eastern Europe and dry over the Mediterranean when NAO is in the positive phase (positive NAO Index, top rows in both cases). The magnitude of these effects is found larger during the negative phase, the changes in temperature being the largest over Scandinavia and the Baltic Sea. Central Europe, the target area in CECILIA, does not present large significant anomalies. The analysis also reveals a good agreement between models.

ii) Future changes (subperiods 1950 -2000, 2001-2050 and 2051-2100)
Comparison of the three sub periods reveals that the above described changes of the same sign and location are found in the future, becoming larger in the course of the 21st century and largest in the last 50-years. The effects were found in average daily mean temperature and in daily maximum and minimum temperatures as well. The effects in daily minimum temperatures are found to cover greater areas. In the case of precipitation, Mediterranean (and its northern surrounding area) is found to become drier for positive changes of NAO Index, while central and northern Europe experience more wet weather.

- Blocking activity
The duration of the blockings did not appear to be as long in the RCMs as in the reanalysis data (ERA40), this being a known feature of the blocking activity simulation in General Circulation Models (GCMs) as well. Our analysis shows significantly lower temperatures and precipitation over central Europe during blockings, while Scandinavia and the Baltic Sea is warmer and drier.

3.11. NIMH

NIMH was involved in all WP4 deliverables except D4.3 and D4.5. It made a significant contribution to the CECILIA extreme database through the computation of indices based on local observations from Bulgaria (see Section 2). For more details on WP4 related analyses and results, please refer to the reports of the respective deliverables.